

755
756
757
758
759
760
761
762
763
764
765
766
767
768
769
770
771
772
773
774
775
776
777

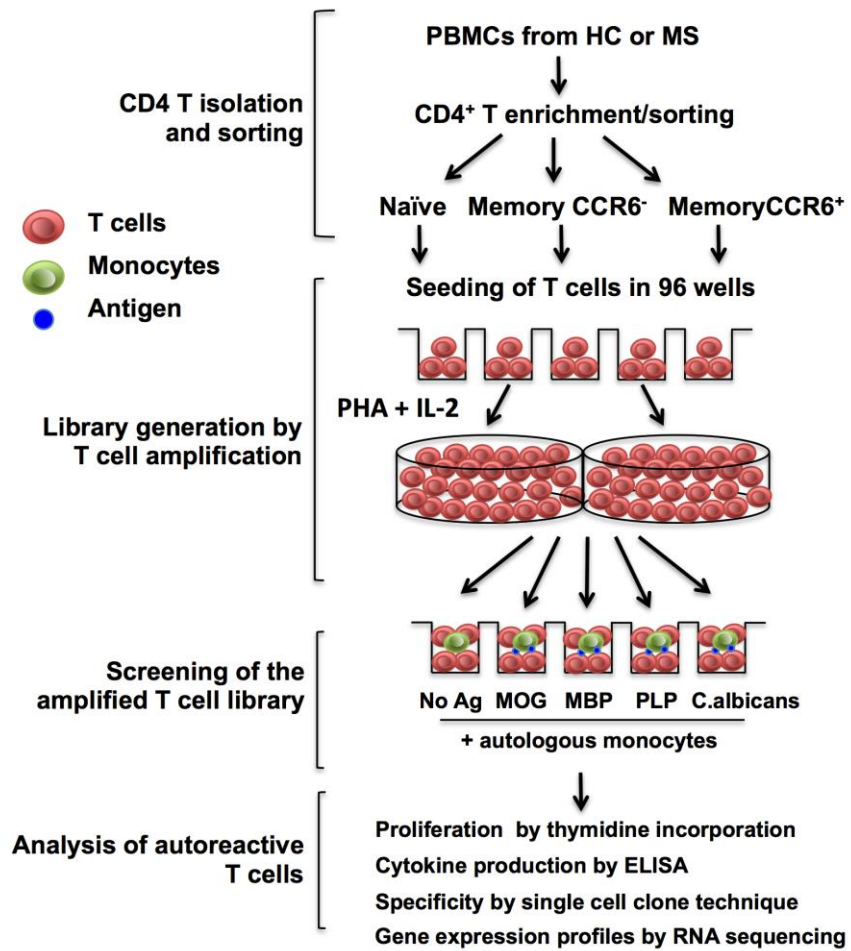
Supplementary Materials for
**Distinct Inflammatory Profiles of Myelin-Reactive T cells from
Patients with Multiple Sclerosis**

Yonghao Cao, Brittany A. Goods, Khadir Raddassi, Gerald T. Nepom,
William W. Kwok, J. Christopher Love, David A. Hafler*

*Corresponding author. Email: david.hafler@yale.edu

This PDF file includes:
Figs. S1 to S16
Tables S1 to S8
References (50-51)

778
779
780
781
782
783
784
785
786
787
788
789
790
791
792
793
794
795
796
797
798
799
800



801 **Fig. S1. Schematic representation of amplified T cell library assay.** Naïve, CCR6⁻ memory
802 and CCR6⁺ memory CD4⁺ T cells from patients with MS or healthy controls (HC) were sorted
803 and seeded at 2,000 cells per well in 96-well plates, and stimulated with PHA and IL-2 in the
804 presence of irradiated allogeneic feeder cells for 2 weeks. After the stimulation cocktail was
805 washed out, the cells from each well were re-stimulated by autologous monocytes and myelin
806 peptides, *C. albicans*. Myelin-specific CD4⁺ T cell proliferation (day 5) and cytokine production
807 (day 7) were measured by ³H-thymidine incorporation and ELISA assay.
808

809
810
811
812
813
814
815
816
817
818
819
820
821
822
823
824
825
826
827
828
829
830
831
832
833
834
835
836

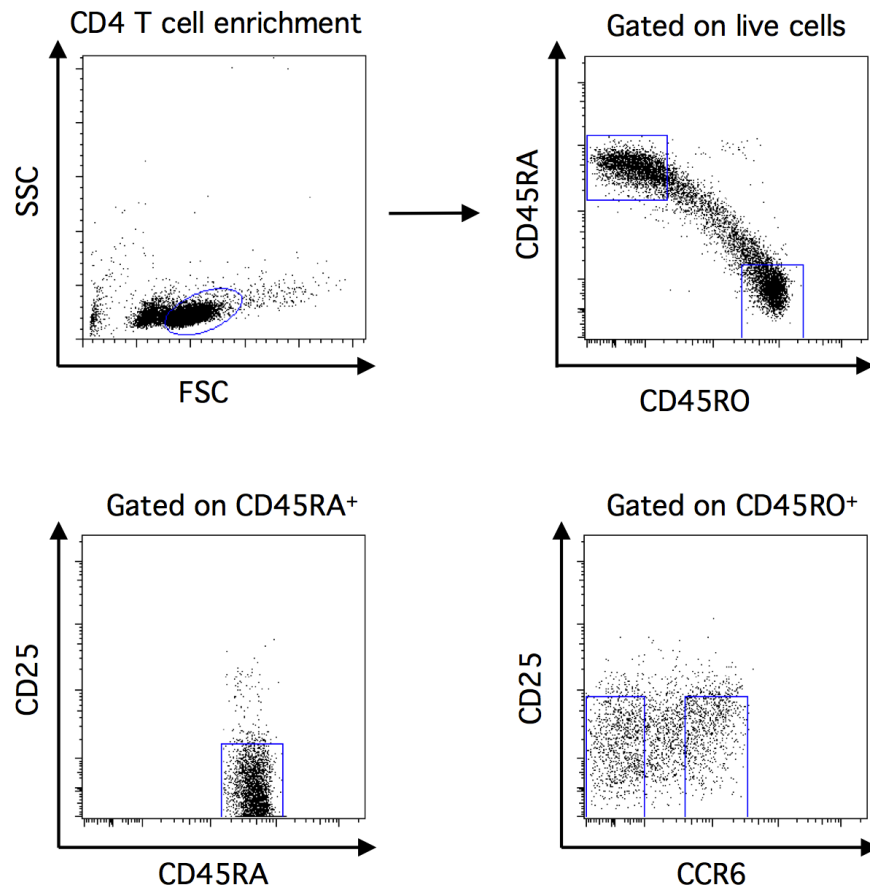
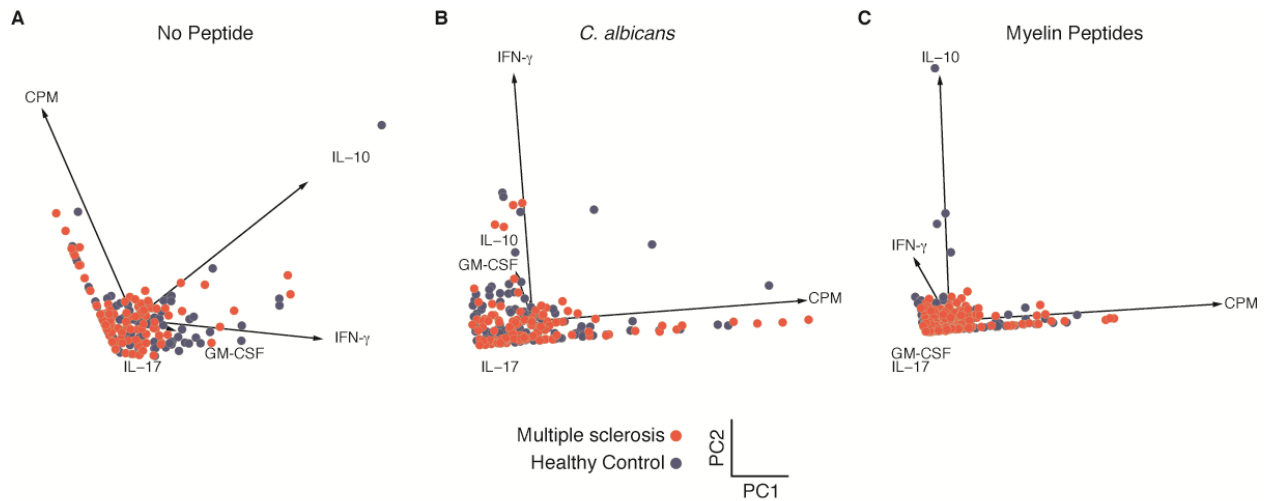


Fig. S2. Sorting strategy of each T cell subpopulation. Total CD4⁺ T cells were enriched by negative selection from PBMCs. Untouched CD4⁺ T cells were stained with monoclonal antibodies against CD45RA, CD45RO, CD25 and CCR6 for T cell subpopulation isolation. The following subpopulations were gated and sorted: Naïve (CD45RA⁺CD45RO⁻CD25⁻), CCR6⁻ memory (CD45RA⁻CD45RO⁺CD25⁻CCR6⁻), and CCR6⁺ memory (CD45RA⁻CD45RO⁺CD25⁻CCR6⁺).

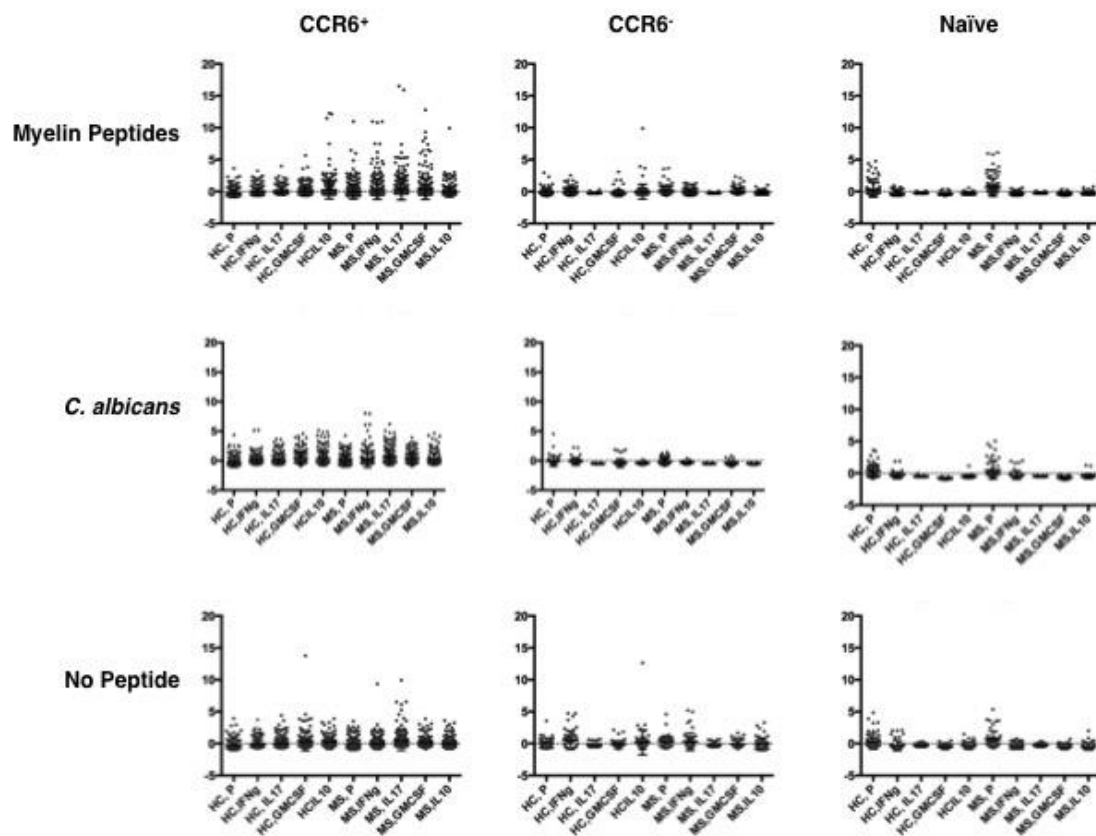
837
838
839



840

841 **Fig. S3. Principal component analysis of functional phenotypes of myelin-reactive**
842 **CD4⁺CCR6⁻ T cells.** Scatterplots show measured penta-dimensional responses (proliferation,
843 IFN- γ , IL-17, GM-CSF and IL-10) for individual amplified T cell libraries (each dot) projected
844 onto the first two principal components. Analysis is shown for (A) no peptide, (B) *C. albicans*,
845 and (C) myelin peptides from eight healthy subjects and eight MS patients. Projections of the
846 vectors for each data class are also shown and annotated for reference. Statistically significant p-
847 values are shown below: *C. albicans*-reactive T cells for proliferation ($p = 0.0017$) and GM-CSF
848 ($p < 0.0001$).
849

850
851
852
853
854
855



856
857
858
859
860
861
862
863

Fig. S4. Functional phenotypes of CCR6⁺ memory, CCR6⁻ memory, and naïve CD4⁺ T cells. Plots show all z –score normalized data for no peptide, *C. albicans*, and myelin peptides corresponding to PCA analysis presented in Figure 2 and Figure S3.

864
865
866
867
868
869
870
871
872
873
874
875
876
877
878
879

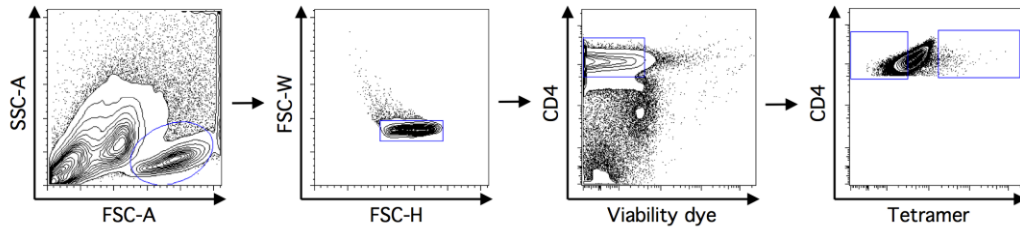
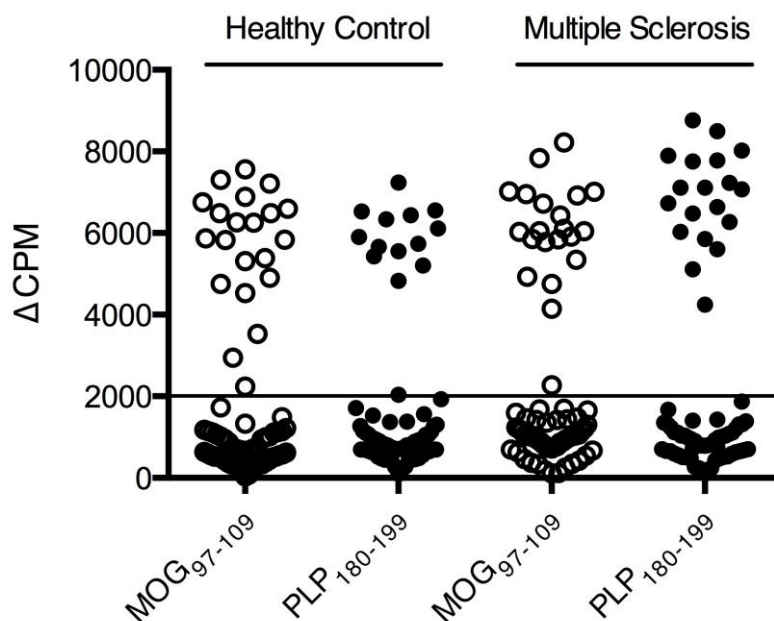


Fig. S5. Representative tetramer staining and sorting strategy of each library from MS patients and healthy controls were chosen for single-cell cloning and RNA sequencing. Two of the highest proliferated wells (red dots shown in fig. S7) were picked and stained by DR4 myelin peptides tetramers (MOG₉₇₋₁₀₉ tetramers and PLP₁₈₀₋₁₉₉ tetramers). MOG₉₇₋₁₀₉ tetramer-positive and PLP₁₈₀₋₁₉₉ tetramer-positive T cells were sorted for single-cell cloning. Tetramer-positive and tetramer-negative T cells were sorted for RNA sequencing.

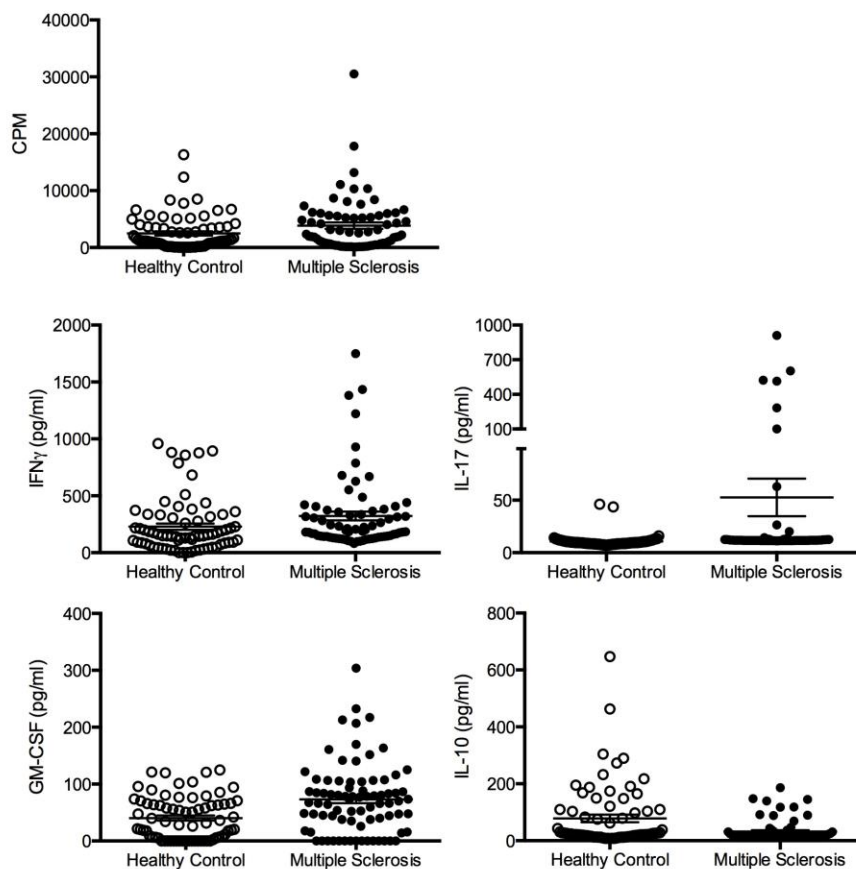
880
881
882
883



884
885
886
887
888
889
890
891
892
893
894

Fig. S6. Specificity of myelin-reactive CD4⁺ T cells. CCR6⁺ memory CD4⁺ T cells from two paired HLA-DR4 healthy subjects and DR4 MS patients were amplified by PHA and IL-2, and scored for proliferation upon re-stimulation with autologous monocytes pulsed with DR4 peptides. The highest sorted wells were used for single-cell sorting using MOG₉₇₋₁₀₉- and PLP₁₈₀₋₁₉₉-tetramers. Single-cell clones were stimulated by monocytes pulsed with no peptide, MOG₉₇₋₁₀₉ or PLP₁₈₀₋₁₉₉. Cell proliferation of each clone was measured on day 5. Dot plots show ΔCPM, which was calculated as peptide pulsed culture CPM – no peptide-pulsed culture CPM. Cultures were scored positive when ΔCPM exceeded 2,000 and the stimulation index was > 3.

895
896
897
898
899
900
901
902
903
904
905
906
907
908
909
910
911
912
913
914
915
916
917
918
919
920



921 **Fig. S7. Phenotypic analysis of myelin-specific single cell clones.** Tetramer-sorted single cell
922 clones (n = 144) were stimulated with DR4 myelin peptides (MOG₉₇₋₁₀₉ and PLP₁₈₀₋₁₉₉) to verify
923 the specificity. The cell proliferation and cytokine production of these clones were measured on
924 day 5 after stimulation. Data were shown as mean \pm SEM. The functional profiles of responsive
925 clones were shown as hierarchical clusters in Figure 3.
926

927
928
929
930
931
932
933
934
935
936
937
938
939
940
941
942
943
944
945
946
947
948
949
950
951
952
953
954
955
956
957

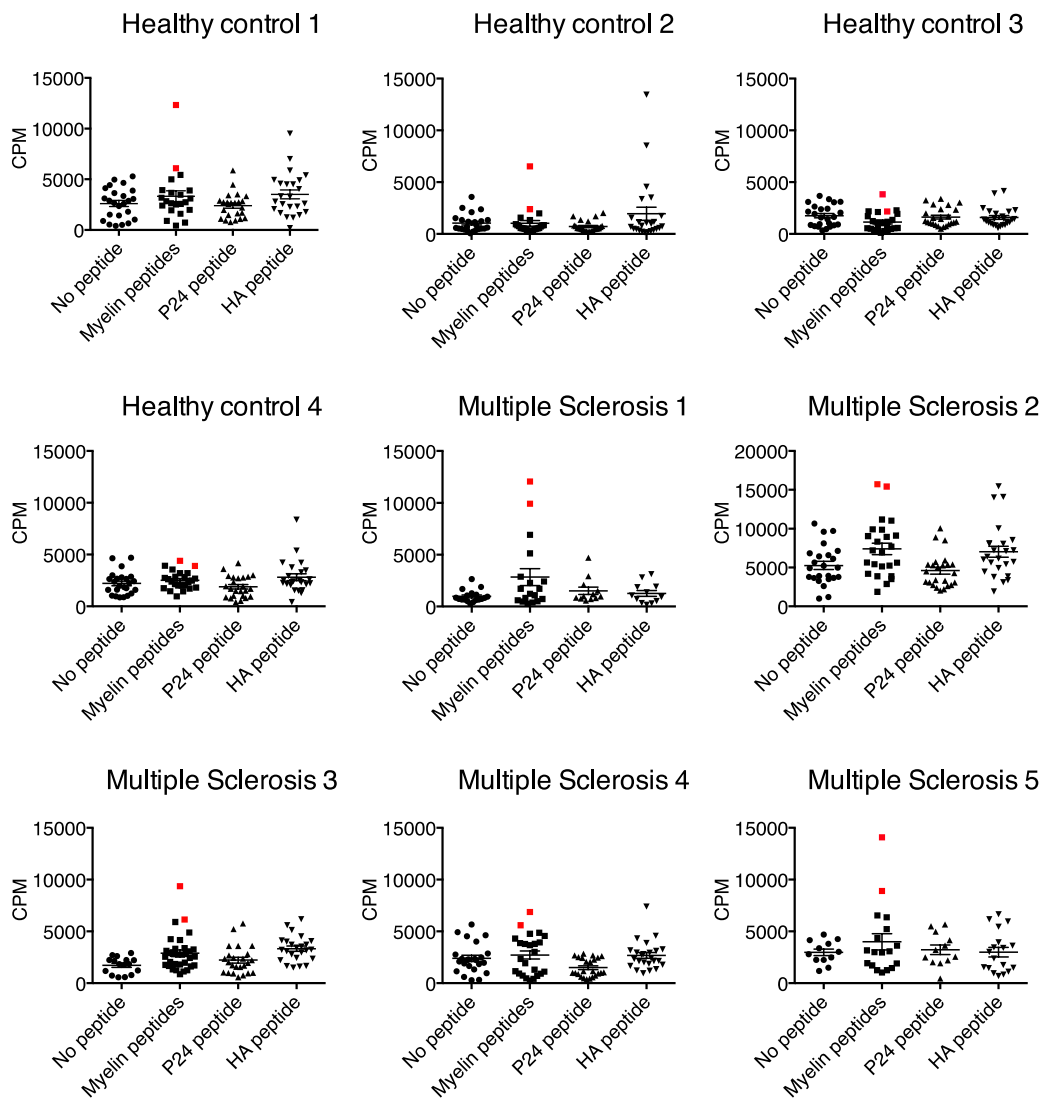
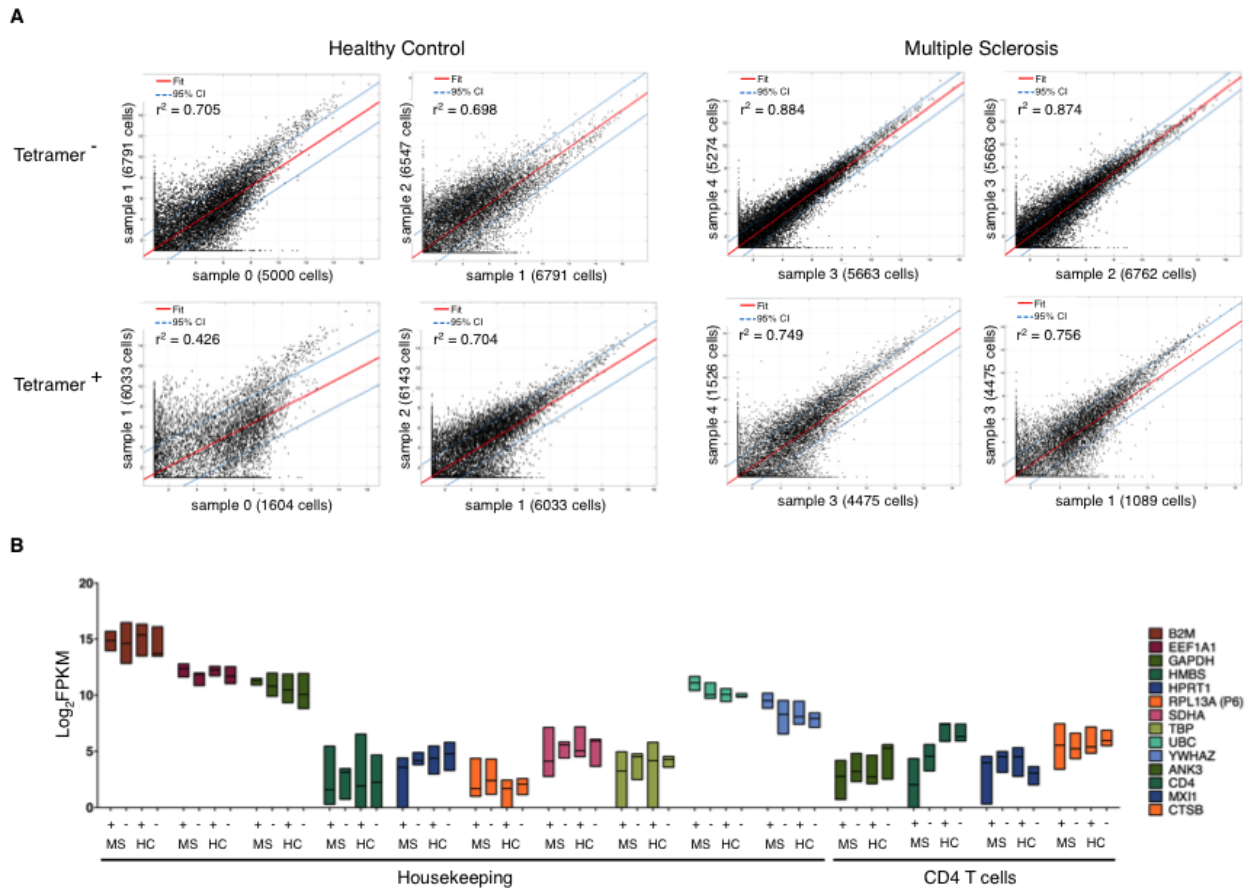
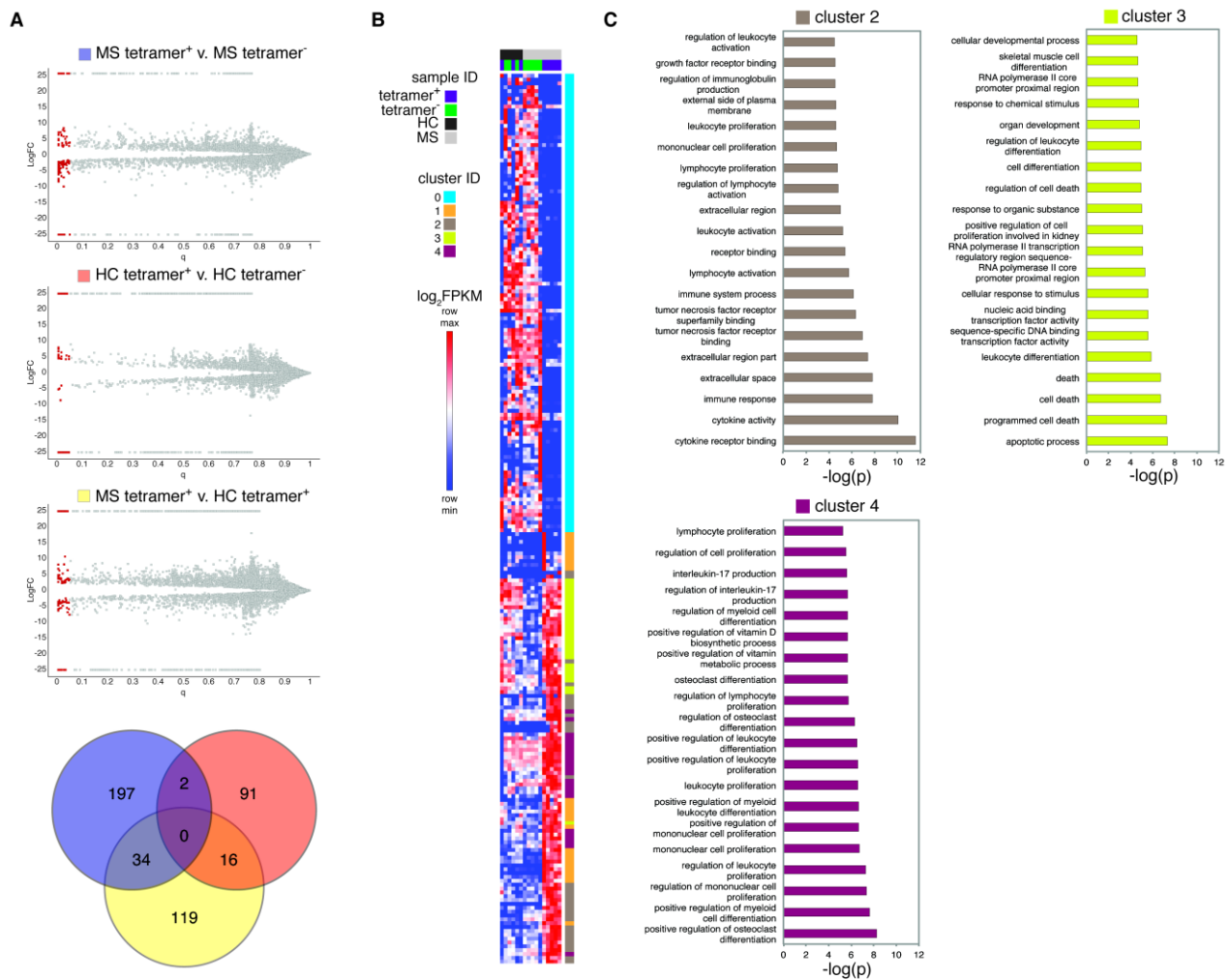


Fig. S8. Cell proliferation of each well from MS patients and healthy controls chosen for RNA sequencing. Four HLA-DR4 healthy controls and five HLA-DR4 MS samples were run. CCR6⁺ memory T cells were amplified by PHA and IL-2 in 96-well plates, and stimulated by irradiated autologous monocytes and DR4 myelin peptides (MOG₉₇₋₁₀₉ and PLP₁₈₀₋₁₉₉). Two of the highest proliferated wells (red dots) of each sample were picked for RNA sequencing. HIV peptide (P24₁₆₆₋₁₉₇) and hemagglutinin peptide (HA₃₀₆₋₃₁₈) used as a negative and positive control.



958
 959
 960
 961
 962
 963
 964
 965
 966
 967
 968
 969

Fig. S9. Correlation of RNA-seq data across biological replicates. (A) Correlation scatter plots of $\log(\text{FPKM}+1)$ values for indicated samples. Linear regression performed in MATLAB using regression toolbox and r^2 values shown. Red lines show the linear fit and blue dotted lines indicate the 95% confidence interval bounds. (B) Box-plots are shown for each sample included in down stream analysis ($n = 3$ HC tetramer⁺ and tetramer⁻, $n = 5$ MS tetramer⁺ and tetramer⁻). Line indicates median, boxes extend to the minimum and maximum of replicates included. Housekeeping (50) and CD4 T cell specific (51) genes are shown.



971
 972
 973
 974
 975
 976
 977
 978
 979
 980
 981

Fig. S10. Differential expression analysis of myelin-reactive T cells in MS and healthy controls. (A) Volcano plots show differentially expressed (DE) genes ($q < 0.05$, red), and Venn diagram shows overlap between DE genes from each comparison purple (MS tetramer⁺ vs. MS tetramer⁻), pink (HC tetramer⁺ vs. HC tetramer⁻), and yellow (MS tetramer⁺ vs. HC tetramer⁺). (B) DE genes unique to MS tetramer⁺ samples were k means clustered for columns ($k = 4$) and rows ($k = 5$) using GeneE. Clusters are shown in colored bars. (C) Genes from each cluster were used to perform GO analysis using FuncAssociate to identify biological functions. $-\log P$ for each function is plotted for clusters that were found to have enriched functions.

982
983
984
985
986
987
988
989
990
991
992
993
994
995
996
997
998
999
1000
1001

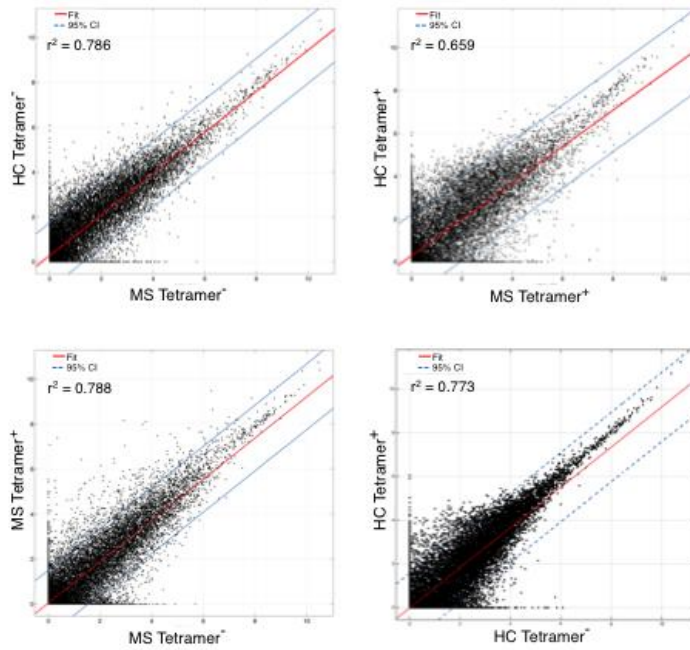


Fig. S11. Correlation scatter plots. Correlation scatter plots of $\log(\text{averageFPKM}+1)$ values for indicated samples. Genes whose expression was zero for all conditions were removed from the data set. Linear regression performed in MATLAB using regression toolbox and r^2 values shown. Red lines show the linear fit and blue dotted lines indicate the 95% confidence interval bounds.

1002
 1003
 1004
 1005
 1006
 1007
 1008
 1009
 1010
 1011
 1012
 1013
 1014
 1015
 1016
 1017
 1018
 1019
 1020
 1021
 1022
 1023
 1024
 1025

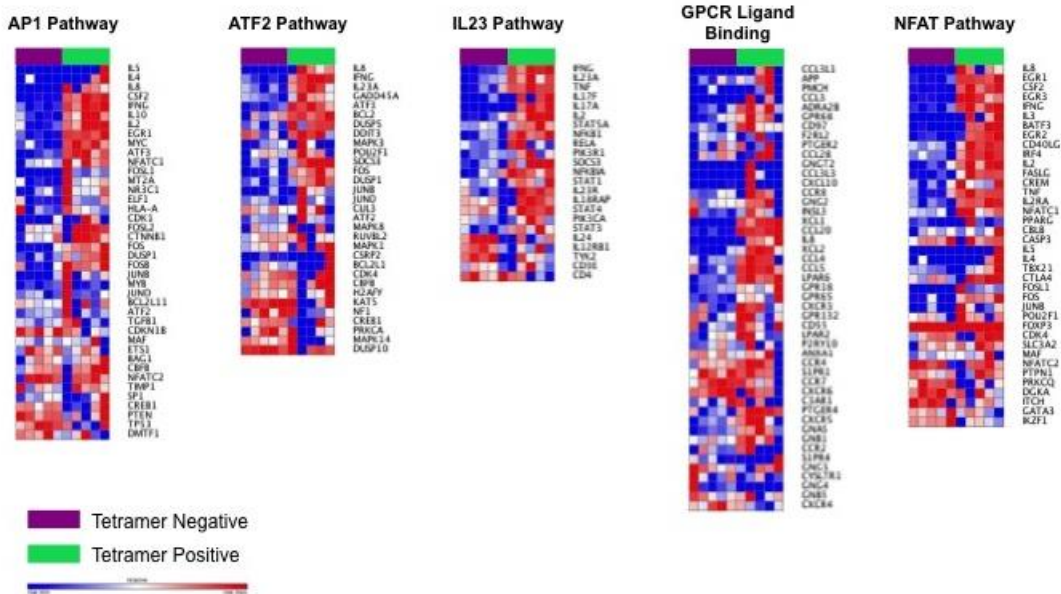
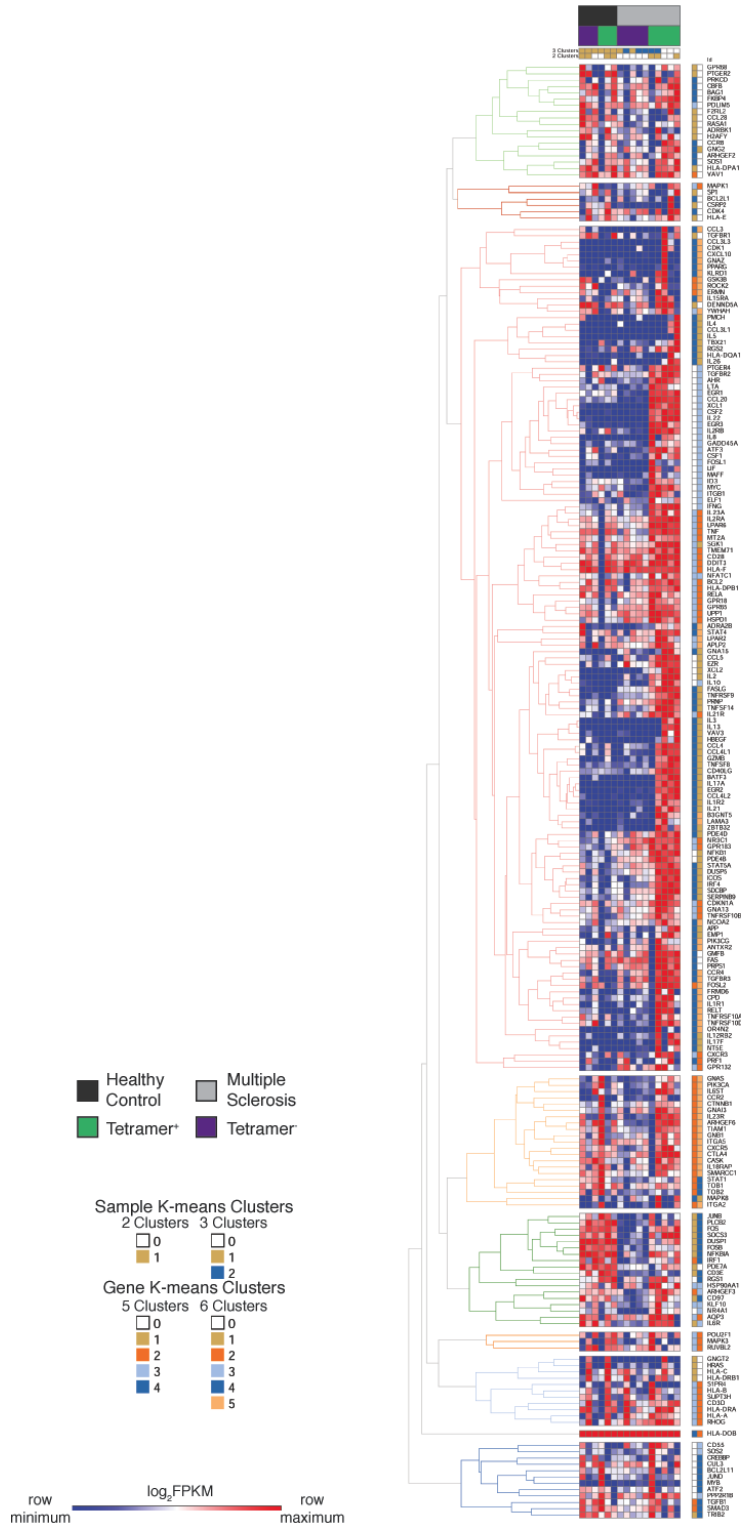
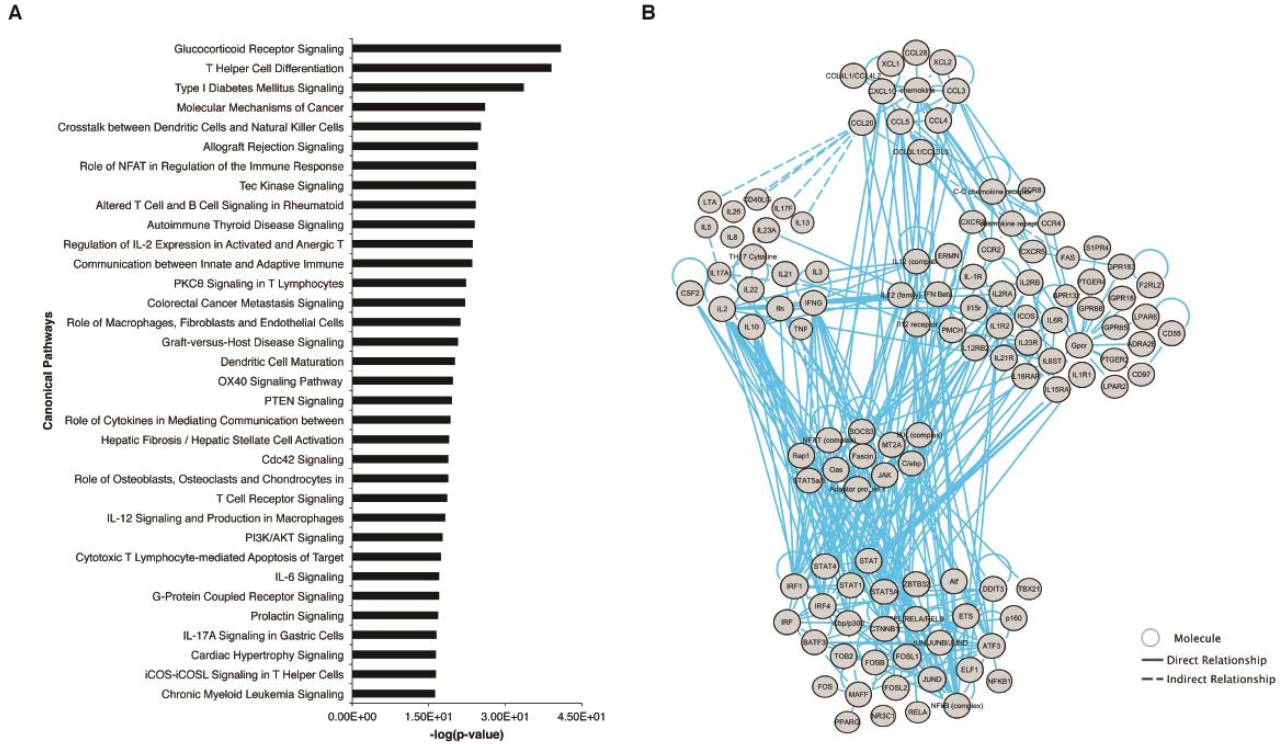


Fig. S12. Heatmaps of selected enriched gene sets identified by GSEA in MS tetramer positive samples. Log₂FPKM values were used to generate each heatmap with GeneE.

1048
1049
1050
1051
1052
1053
1054
1055
1056
1057
1058
1059
1060
1061
1062
1063
1064
1065
1066
1067
1068
1069
1070
1071
1072
1073
1074
1075
1076
1077

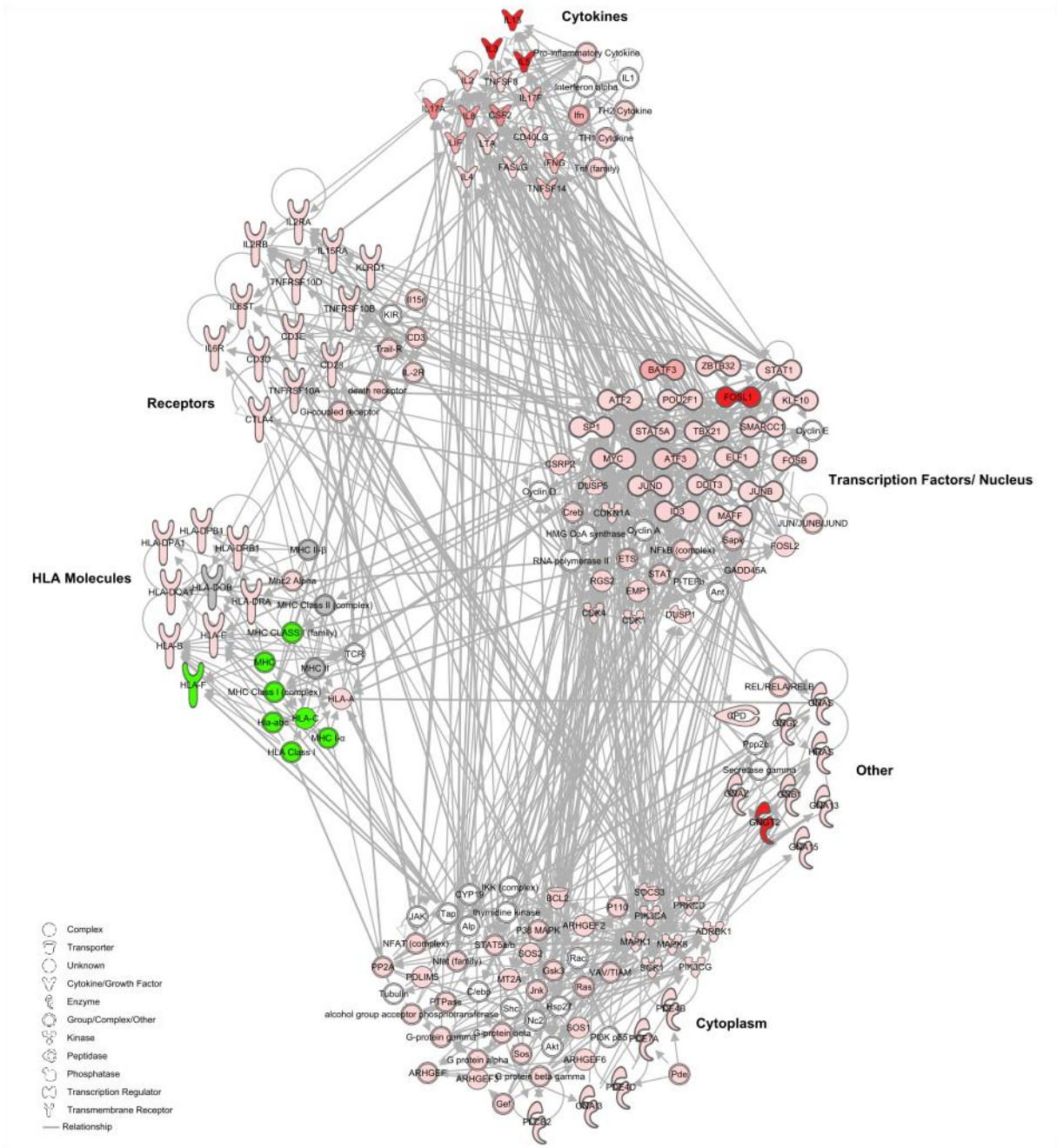


1078 **Fig. S14. Heatmap of log₂FPKM values for the 224-gene leading edge set.** Data are shown for
 1079 all samples passing quality control filters. Data were clustered hierarchically (dendrogram) row-
 1080 wise and by k means for columns (k = 2 and k = 3) and rows (k = 5 and k = 6) using GeneE.



1081
 1082
 1083
 1084
 1085
 1086
 1087
 1088
 1089
 1090
 1091
 1092
 1093

Fig. S15. Enriched canonical pathways and network analysis. (A) The top 45 canonical pathways identified as up-regulated in MS tetramer positive samples are plotted as a function of $-\log(p\text{-value})$. Canonical pathways were predicted using IPA and the 235-gene signature. (B) Fully labeled version of network diagram presented in figure 4C. Molecules are represented by circles and relationships represented by dashed (indirect) or solid (direct) cyan lines.



1095
 1096
 1097
 1098
 1099
 1100
 1101
 1102
 1103
 1104

Fig. S16. Additional network analysis. Networks 3-7 from IPA were merged and grouped according to molecular function. Molecules are colored according to logFC(MS^+/MS^-), where red is increased in MS tetramer positive and green in decreased in MS tetramer positive.

Table S1: Patients with MS and paired healthy subjects Information.

| Sample ID | Age | Gender | EDSS Score | Date of first Symptoms | Treatment | Experiment used | T cell libraries generated | | |
|-----------|-----|--------|------------|------------------------|-----------|----------------------|----------------------------|--------------------------|--------------------------|
| | | | | | | | Naïve | CCR6 ⁻ memory | CCR6 ⁺ memory |
| MS128 | 35 | F | 4.0 | 2011 | Untreated | T cell library assay | 192 | 192 | 192 |
| MS168 | 53 | F | N.I. | N.I. | Untreated | T cell library assay | 96 | 96 | 96 |
| MS174 | 45 | F | 1.0 | 2005 | Untreated | T cell library assay | 96 | 96 | 96 |
| MS176 | 53 | F | 1.0 | N.I. | Untreated | T cell library assay | 96 | 96 | 96 |
| MS189 | 61 | F | 1.0 | 2007 | Untreated | T cell library assay | 96 | 96 | 96 |
| MS192 | 33 | M | 1.0 | 2011 | Untreated | T cell library assay | 96 | 96 | 96 |
| MS224 | 25 | F | 1.0 | 2011 | Untreated | T cell library assay | 96 | 96 | 96 |
| MS226 | 57 | F | 2.0 | 2011 | Untreated | T cell library assay | 96 | 96 | 96 |
| MS234 | 20 | F | 1.0 | 2011 | Untreated | T cell library assay | 96 | 96 | 96 |
| MS339 | 29 | M | 1.0 | 2011 | Untreated | T cell library assay | 96 | 96 | 96 |
| MS464 | 37 | M | 2.0 | 2014 | Untreated | T cell library assay | 96 | 96 | 192 |
| MS466 | 51 | F | 1.0 | 2000 | Untreated | T cell library assay | 96 | 96 | 192 |
| MS468 | 33 | F | 2.0 | 2012 | Untreated | T cell library assay | 96 | 96 | 192 |
| MS470 | 47 | M | 1.0 | 1995 | Untreated | T cell library assay | 96 | 96 | 192 |
| MS472 | 32 | F | 3.0 | 2014 | Untreated | T cell library assay | 96 | 96 | 192 |
| MS333 | 29 | M | 1.0 | 2012 | Untreated | Single cell cloning | 66 | 68 | 192 |
| MS304 | 39 | M | 1.0 | 2002 | Untreated | Single cell cloning | 0 | 0 | 192 |
| MS361 | 40 | M | 1.0 | 2013 | Untreated | Single cell cloning | 0 | 0 | 192 |
| MS181 | 64 | F | 6.5 | 2000 | Untreated | RNA sequencing | 0 | 0 | 192 |
| MS266 | 57 | F | 2.0 | 1985 | Untreated | RNA sequencing | 0 | 0 | 192 |
| MS386 | 48 | F | 6.0 | 1994 | Untreated | RNA sequencing | 0 | 0 | 192 |
| MS358 | 50 | F | 1.0 | 2013 | Untreated | RNA sequencing | 0 | 0 | 192 |
| MS369 | 43 | M | 3.0 | 2013 | Untreated | RNA sequencing | 0 | 0 | 192 |

1107

Table S1: Patients with MS and paired healthy subjects Information (continued).

| Sample ID | Age | Gender | EDSS Score | Date of first Symptoms | Treatment | Experiment used | T cell libraries generated | | |
|-----------|-----|--------|------------|------------------------|-----------|----------------------|----------------------------|--------------------------|--------------------------|
| | | | | | | | Naïve | CCR6 ⁻ memory | CCR6 ⁺ memory |
| HC292 | 31 | M | N.A. | N.A. | N.A. | T cell library assay | 192 | 192 | 192 |
| HC304 | 50 | M | N.A. | N.A. | N.A. | T cell library assay | 96 | 96 | 96 |
| HC309 | 32 | M | N.A. | N.A. | N.A. | T cell library assay | 96 | 96 | 96 |
| HC293 | 25 | F | N.A. | N.A. | N.A. | T cell library assay | 96 | 96 | 96 |
| HC326 | 34 | M | N.A. | N.A. | N.A. | T cell library assay | 96 | 96 | 96 |
| HC322 | 39 | M | N.A. | N.A. | N.A. | T cell library assay | 96 | 96 | 96 |
| HC301 | 27 | F | N.A. | N.A. | N.A. | T cell library assay | 96 | 96 | 96 |
| HC310 | 32 | M | N.A. | N.A. | N.A. | T cell library assay | 96 | 96 | 96 |
| HC298 | 39 | F | N.A. | N.A. | N.A. | T cell library assay | 96 | 96 | 96 |
| HC300 | 54 | F | N.A. | N.A. | N.A. | T cell library assay | 96 | 96 | 96 |
| HC2614 | 30 | M | N.A. | N.A. | N.A. | T cell library assay | 96 | 96 | 192 |
| HC2623 | 46 | F | N.A. | N.A. | N.A. | T cell library assay | 96 | 96 | 192 |
| HC2613 | 22 | F | N.A. | N.A. | N.A. | T cell library assay | 96 | 96 | 192 |
| HC2618 | 52 | M | N.A. | N.A. | N.A. | T cell library assay | 96 | 96 | 192 |
| HC2622 | 28 | F | N.A. | N.A. | N.A. | T cell library assay | 96 | 96 | 192 |
| HC226 | 31 | M | N.A. | N.A. | N.A. | Single cell cloning | 66 | 68 | 192 |
| HC310 | 32 | M | N.A. | N.A. | N.A. | Single cell cloning | 0 | 0 | 192 |
| HC333 | 52 | M | N.A. | N.A. | N.A. | Single cell cloning | 0 | 0 | 192 |
| HC391 | 35 | M | N.A. | N.A. | N.A. | RNA sequencing | 0 | 0 | 192 |
| HC311 | 32 | M | N.A. | N.A. | N.A. | RNA sequencing | 0 | 0 | 192 |
| HC322 | 37 | M | N.A. | N.A. | N.A. | RNA sequencing | 0 | 0 | 192 |
| HC330 | 52 | M | N.A. | N.A. | N.A. | RNA sequencing | 0 | 0 | 192 |

1108

1109 N.I., no information available;

1110 N.A., not applicable.

1111

1112
 1113
 1114
 1115
 1116

Table S2. Myelin peptides and control peptides used in T cell library assays.

| Peptides | Sequences | Tetramers |
|------------------------|----------------------|----------------------------------|
| MBP ₈₅₋₉₉ | NPVVHFFKNIVTPRT | DRB1*1501/MBP ₈₅₋₉₉ |
| MOG ₂₂₂₋₂₄₁ | VALIICYNWLHRRLAGQFLE | DRB1*1501/MOG ₂₂₂₋₂₄₁ |
| PLP ₃₀₋₄₉ | ALFCGCGHEALTGTEKLIET | DRB1*1501/PLP ₃₀₋₄₉ |
| PLP ₁₂₉₋₁₄₈ | QHQAHS�ERVCHCLGKWLGH | DRB1*1501/PLP ₁₂₉₋₁₄₈ |
| MOG ₉₇₋₁₀₉ | RTELLKDAIGEGK | DRB1*0401/MOG ₉₇₋₁₀₉ |
| PLP ₁₈₀₋₁₉₉ | TWTTCQSIAPSKTSASIGS | DRB1*0401/PLP ₁₈₀₋₁₉₉ |
| HA ₃₀₆₋₃₁₈ | PRYVKQNTLKLAT | / |
| P24 ₁₆₆₋₁₇₉ | DRFYKTLRAEQASQ | / |

1117
 1118
 1119
 1120
 1121
 1122
 1123
 1124
 1125
 1126
 1127
 1128
 1129
 1130
 1131
 1132
 1133
 1134
 1135
 1136
 1137
 1138
 1139
 1140
 1141

Abbreviations: MBP, myelin basic protein; MOG, myelin oligodendrocyte glycoprotein; PLP, proteolipid protein; HA, hemagglutinin.

1142
1143
1144

Table S3. Percent variance explained by each principal component.

| Condition | <i>C. albicans</i> | | No peptide | | Myelin peptides | |
|------------------|-----------------------------|-------------------|-----------------------------|-------------------|-----------------------------|-------------------|
| | Naïve/ CCR6 ⁻ | CCR6 ⁺ | Naïve/ CCR6 ⁻ | CCR6 ⁺ | Naïve/ CCR6 ⁻ | CCR6 ⁺ |
| PC1 | 66.91 | 30.67 | 48.26 | 33.57 | 58.15 | 33.16 |
| PC2 | 16.92 | 23.54 | 27.00 | 26.66 | 21.58 | 22.41 |
| PC3 | 12.37 | 20.68 | 17.77 | 16.99 | 10.80 | 21.14 |
| PC4 | 3.48 | 15.05 | 5.52 | 12.89 | 8.98 | 14.64 |
| PC5 | 0.32 | 10.06 | 1.45 | 9.89 | 0.49 | 8.64 |

1145
1146

1147 **Table S4. GSEA results (FDR < 0.25) for comparison of MS tetramer positive to MS**
 1148 **tetramer negative.**
 1149

| NAME | NES | NOM p-val | FDR q-val |
|--|-------|-----------|-----------|
| KEGG_CYTOKINE_CYTOKINE_RECEPTOR_INTERACTION | 5.255 | <0.001 | <0.001 |
| REACTOME_3_UTR_MEDIATED_TRANSLATIONAL_REGULATION | 4.418 | <0.001 | <0.001 |
| MIPS_RIBOSOME_CYTOPLASMIC | 4.120 | <0.001 | <0.001 |
| MIPS_NOP56P_ASSOCIATED_PRE_RRNA_COMPLEX | 3.941 | <0.001 | <0.001 |
| KEGG_RIBOSOME | 3.848 | <0.001 | <0.001 |
| REACTOME_PEPTIDE_CHAIN_ELONGATION | 3.798 | <0.001 | <0.001 |
| PID_NFAT_TFPATHWAY | 3.797 | <0.001 | <0.001 |
| REACTOME_NONSENSE_MEDIATED_DECAY_ENHANCED_BY_THE_EXON_JUNCTION_COMPLEX | 3.676 | <0.001 | <0.001 |
| BIOCARTA_CYTOKINE_PATHWAY | 3.599 | <0.001 | <0.001 |
| REACTOME_GPCR_LIGAND_BINDING | 3.534 | <0.001 | <0.001 |
| REACTOME_CLASS_A1_RHODOPSIN_LIKE_RECEPTORS | 3.497 | <0.001 | <0.001 |
| REACTOME_TRANSLATION | 3.452 | <0.001 | <0.001 |
| REACTOME_ACTIVATION_OF_THE_MRNA_UPON_BINDING_OF_THE_CAP_BINDING_COMPLEX_AND_EIF5_AND_SUBSEQUENT_BINDING_TO_43S | 3.351 | <0.001 | <0.001 |
| PID_API_PATHWAY | 3.319 | <0.001 | <0.001 |
| PID_ATF2_PATHWAY | 3.213 | <0.001 | <0.001 |
| BIOCARTA_INFLAM_PATHWAY | 3.182 | <0.001 | <0.001 |
| REACTOME_INFLUENZA_VIRAL_RNA_TRANSCRIPTION_AND_REPLICATION | 3.177 | <0.001 | <0.001 |
| MIPS_60S_RIBOSOMAL_SUBUNIT_CYTOPLASMIC | 3.158 | <0.001 | <0.001 |
| REACTOME_FORMATION_OF_THE_TERNARY_COMPLEX_AND_SUBSEQUENTLY_THE_43S_COMPLEX | 3.140 | <0.001 | 0.0001 |
| REACTOME_GPCR_DOWNSTREAM_SIGNALING | 3.112 | <0.001 | 0.0001 |
| REACTOME_INFLUENZA_LIFE_CYCLE | 3.064 | <0.001 | 0.0001 |
| REACTOME_SIGNALING_BY_GPCR | 3.047 | <0.001 | 0.0001 |
| REACTOME_CHEMOKINE_RECEPTORS_BIND_CHEMOKINES | 3.043 | <0.001 | 0.0001 |
| PID_TCR_CALCIUM_PATHWAY | 2.993 | <0.001 | 0.0001 |
| KEGG_CHEMOKINE_SIGNALING_PATHWAY | 2.878 | <0.001 | 0.0001 |
| REACTOME_PEPTIDE_LIGAND_BINDING_RECEPTORS | 2.874 | <0.001 | 0.0001 |
| KEGG_ASTHMA | 2.804 | <0.001 | 0.0002 |
| PID_IL23_PATHWAY | 2.790 | <0.001 | 0.0002 |
| KEGG_ALLOGRAFT_REJECTION | 2.772 | <0.001 | 0.0002 |
| PID_REG_GR_PATHWAY | 2.769 | <0.001 | 0.0002 |
| KEGG_AUTOIMMUNE_THYROID_DISEASE | 2.707 | <0.001 | 0.0005 |
| REACTOME_METABOLISM_OF_PROTEINS | 2.691 | <0.001 | 0.0005 |
| KEGG_MAPK_SIGNALING_PATHWAY | 2.690 | <0.001 | 0.0005 |
| KEGG_JAK_STAT_SIGNALING_PATHWAY | 2.663 | <0.001 | 0.0007 |
| BIOCARTA_NKT_PATHWAY | 2.636 | <0.001 | 0.0008 |
| KEGG_TYPE_I_DIABETES_MELLITUS | 2.636 | <0.001 | 0.0008 |
| REACTOME_METABOLISM_OF_RNA | 2.598 | <0.001 | 0.0013 |
| REACTOME_SIGNALING_BY_ILS | 2.583 | <0.001 | 0.0013 |

| | | | |
|--|-------|--------|--------|
| KEGG_GRAFT_VERSUS_HOST_DISEASE | 2.579 | <0.001 | 0.0013 |
| MIPS_40S_RIBOSOMAL_SUBUNIT_CYTOPLASMIC | 2.565 | <0.001 | 0.0014 |
| BIOCARTA_MET_PATHWAY | 2.534 | <0.001 | 0.0018 |
| REACTOME_SLC_MEDIATED_TRANSMEMBRANE_TRANSPORT | 2.505 | <0.001 | 0.0020 |
| BIOCARTA_TFF_PATHWAY | 2.497 | <0.001 | 0.0021 |
| REACTOME_METABOLISM_OF_MRNA | 2.493 | <0.001 | 0.0022 |
| BIOCARTA_NTHI_PATHWAY | 2.484 | <0.001 | 0.0022 |
| KEGG_HEMATOPOIETIC_CELL_LINEAGE | 2.466 | <0.001 | 0.0025 |
| BIOCARTA_DC_PATHWAY | 2.462 | <0.001 | 0.0025 |
| PID_MYC_ACTIVPATHWAY | 2.447 | <0.001 | 0.0028 |
| PID_IL12_2PATHWAY | 2.415 | <0.001 | 0.0038 |
| PID_ECADHERIN_STABILIZATION_PATHWAY | 2.396 | <0.001 | 0.0044 |
| PID_IL2_STAT5PATHWAY | 2.379 | 0.0019 | 0.0051 |
| PID_INTEGRIN1_PATHWAY | 2.375 | <0.001 | 0.0051 |
| KEGG_PATHWAYS_IN_CANCER | 2.371 | <0.001 | 0.0053 |
| REACTOME_TRANSPORT_OF_INORGANIC_CATIONS_ANIONS_AND_AMINO_ACIDS_OLIGOPEPTIDES | 2.365 | 0.0020 | 0.0055 |
| KEGG_SYSTEMIC_LUPUS_ERYTHEMATOSUS | 2.359 | <0.001 | 0.0056 |
| PID_HIF1_TFPATHWAY | 2.343 | 0.0019 | 0.0062 |
| KEGG_T_CELL_RECEPTOR_SIGNALING_PATHWAY | 2.332 | <0.001 | 0.0064 |
| KEGG_SMALL_CELL_LUNG_CANCER | 2.305 | 0.0020 | 0.0077 |
| BIOCARTA_AKT_PATHWAY | 2.272 | 0.0019 | 0.0095 |
| REACTOME_PLATELET_ACTIVATION_SIGNALING_AND_AGGREGATION | 2.270 | 0.0060 | 0.0094 |
| MIPS_EIF3_COMPLEX | 2.265 | <0.001 | 0.0097 |
| MIPS_CHUK_NFKB2_REL_IKBKG_SPAG9_NFKB1_NFKBIE_COPB2_TNIP1_NFKBIA_RELA_TNIP2_COMPLEX | 2.264 | <0.001 | 0.0096 |
| BIOCARTA_GCR_PATHWAY | 2.211 | 0.0020 | 0.0141 |
| REACTOME_CYTOKINE_SIGNALING_IN_IMMUNE_SYSTEM | 2.209 | 0.0019 | 0.0140 |
| PID_AVB3_OPN_PATHWAY | 2.207 | <0.001 | 0.0140 |
| KEGG_ADHERENS_JUNCTION | 2.191 | <0.001 | 0.0154 |
| KEGG_SPLICEOSOME | 2.187 | 0.0020 | 0.0156 |
| PID_IL6_7PATHWAY | 2.183 | <0.001 | 0.0157 |
| PID_PDGFBRBPATHWAY | 2.173 | 0.0020 | 0.0165 |
| PID_CD8TCRDOWNSTREAMPATHWAY | 2.170 | 0.0058 | 0.0165 |
| REACTOME_G_ALPHA_I_SIGNALLING_EVENTS | 2.166 | <0.001 | 0.0166 |
| PID_AJDISS_2PATHWAY | 2.159 | 0.0020 | 0.0170 |
| PID_NFKAPPABCANONICALPATHWAY | 2.156 | 0.0062 | 0.0171 |
| KEGG_REGULATION_OF_ACTIN_CYTOSKELETON | 2.143 | 0.0019 | 0.0185 |
| BIOCARTA_IGF1_PATHWAY | 2.139 | <0.001 | 0.0188 |
| KEGG_INTESTINAL_IMMUNE_NETWORK_FOR_IGA_PRODUCTION | 2.134 | <0.001 | 0.0191 |
| PID_IL12_STAT4PATHWAY | 2.130 | 0.0038 | 0.0194 |
| MIPS_TRBP_CONTAINING_COMPLEX_1 | 2.115 | 0.0019 | 0.0213 |
| PID_IL2_1PATHWAY | 2.114 | <0.001 | 0.0211 |
| MIPS_17S_U2_SNRNP | 2.109 | 0.0020 | 0.0218 |

| | | | |
|--|-------|--------|--------|
| BIOCARTA_IL2RB_PATHWAY | 2.104 | 0.0042 | 0.0220 |
| KEGG_ANTIGEN_PROCESSING_AND_PRESENTATION | 2.104 | <0.001 | 0.0219 |
| PID_ANGIOPOIETINRECEPTOR_PATHWAY | 2.102 | 0.0020 | 0.0217 |
| PID_ER_NONGENOMIC_PATHWAY | 2.101 | <0.001 | 0.0215 |
| PID_SYNDECAN_2_PATHWAY | 2.099 | 0.0020 | 0.0215 |
| REACTOME_AMINO_ACID_AND_OLIGOPEPTIDE_SLC_TRANSPORTERS | 2.089 | 0.0021 | 0.0228 |
| KEGG_ECM_RECEPTOR_INTERACTION | 2.089 | <0.001 | 0.0226 |
| KEGG_NOD_LIKE_RECEPTOR_SIGNALING_PATHWAY | 2.082 | 0.0039 | 0.0233 |
| BIOCARTA_TOB1_PATHWAY | 2.079 | <0.001 | 0.0234 |
| PID_CD40_PATHWAY | 2.075 | 0.0038 | 0.0238 |
| KEGG_CHRONIC_MYELOID_LEUKEMIA | 2.073 | 0.0019 | 0.0239 |
| MIPS_TNF_ALPHA_NF_KAPPA_B_SIGNALING_COMPLEX | 2.072 | 0.0041 | 0.0238 |
| PID_REELINPATHWAY | 2.071 | 0.0019 | 0.0236 |
| PID_P53REGULATIONPATHWAY | 2.066 | <0.001 | 0.0242 |
| SIG_CD40PATHWAYMAP | 2.066 | 0.0019 | 0.0240 |
| PID_KITPATHWAY | 2.052 | 0.0040 | 0.0258 |
| BIOCARTA_INSULIN_PATHWAY | 2.050 | 0.0102 | 0.0261 |
| PID_EPOPATHWAY | 2.049 | 0.0020 | 0.0259 |
| REACTOME_GROWTH_HORMONE_RECEPTOR_SIGNALING | 2.030 | 0.0020 | 0.0292 |
| PID_TELOMERASEPATHWAY | 2.027 | 0.0020 | 0.0295 |
| REACTOME_HEMOSTASIS | 2.026 | 0.0039 | 0.0294 |
| KEGG_NATURAL_KILLER_CELL_MEDIATED_CYTOTOXICITY | 2.023 | 0.0020 | 0.0296 |
| PID_ERBB1_RECEPTOR_PROXIMAL_PATHWAY | 2.022 | 0.0020 | 0.0295 |
| KEGG_TYPE_II_DIABETES_MELLITUS | 2.016 | 0.0061 | 0.0306 |
| PID_IL27PATHWAY | 2.013 | 0.0126 | 0.0310 |
| KEGG_FOCAL_ADHESION | 2.011 | 0.0062 | 0.0314 |
| KEGG_RIG_I_LIKE_RECEPTOR_SIGNALING_PATHWAY | 2.005 | 0.0063 | 0.0320 |
| KEGG_FC_EPSILON_RI_SIGNALING_PATHWAY | 2.005 | 0.0059 | 0.0319 |
| REACTOME_AXON_GUIDANCE | 2.003 | 0.0038 | 0.0319 |
| PID_SHP2_PATHWAY | 2.002 | 0.0040 | 0.0318 |
| PID_FRA_PATHWAY | 1.998 | 0.0105 | 0.0322 |
| PID_AVB3_INTEGRIN_PATHWAY | 1.994 | 0.0058 | 0.0329 |
| BIOCARTA_NFAT_PATHWAY | 1.986 | 0.0039 | 0.0339 |
| BIOCARTA_41BB_PATHWAY | 1.986 | 0.0042 | 0.0336 |
| KEGG_TOLL_LIKE_RECEPTOR_SIGNALING_PATHWAY | 1.966 | 0.0019 | 0.0375 |
| KEGG_ARGININE_AND_PROLINE_METABOLISM | 1.963 | 0.0062 | 0.0378 |
| REACTOME_NFKB_AND_MAP_KINASES_ACTIVATION_MEDIATED_BY_TLR4_SIGNALING_REPEAT | 1.958 | 0.0059 | 0.0385 |
| REACTOME_IL_3_5_AND_GM-CSF_SIGNALING | 1.958 | 0.0079 | 0.0383 |
| REACTOME_TRIGLYCERIDE_BIOSYNTHESIS | 1.955 | 0.0104 | 0.0385 |
| KEGG_LEISHMANIA_INFECTION | 1.954 | 0.0039 | 0.0385 |
| REACTOME_MYD88_MAL_CASCADE_INITIATED_ON_PLASMA_MEMBRANE | 1.945 | 0.0120 | 0.0406 |
| REACTOME_TRANSPORT_OF_MATURE_TRANSCRIPT_TO_CYTOPLASM | 1.933 | 0.0108 | 0.0430 |

| | | | |
|---|-------|--------|--------|
| PID_LYSOPHOSPHOLIPID_PATHWAY | 1.932 | 0.0084 | 0.0427 |
| BIOCARTA_PPARA_PATHWAY | 1.928 | 0.0141 | 0.0435 |
| REACTOME_TAK1_ACTIVATES_NFKB_BY_PHOSPHORYLATION_AND_ACTIVATION_OF_IKKS_COMPLEX | 1.927 | 0.0173 | 0.0435 |
| BIOCARTA_EIF_PATHWAY | 1.925 | 0.0078 | 0.0436 |
| PID_RHOA_PATHWAY | 1.923 | 0.0060 | 0.0436 |
| BIOCARTA_IL1R_PATHWAY | 1.920 | 0.0058 | 0.0441 |
| PID_BCR_5PATHWAY | 1.904 | 0.0122 | 0.0485 |
| MIPS_LARGE_DROSHA_COMPLEX | 1.901 | 0.0079 | 0.0489 |
| PID_SYNDECAN_4_PATHWAY | 1.899 | 0.0082 | 0.0490 |
| REACTOME_TRANSMEMBRANE_TRANSPORT_OF_SMALL_MOLECULES | 1.892 | 0.0081 | 0.0507 |
| BIOCARTA_BAD_PATHWAY | 1.891 | 0.0134 | 0.0505 |
| PID_ERBB1_DOWNSTREAM_PATHWAY | 1.889 | 0.0081 | 0.0506 |
| REACTOME_MAP_KINASE_ACTIVATION_IN_TLR_CASCADE | 1.888 | 0.0064 | 0.0507 |
| REACTOME_G_ALPHA_Q_SIGNALLING_EVENTS | 1.884 | 0.0065 | 0.0513 |
| PID_AR_TF_PATHWAY | 1.880 | 0.0156 | 0.0519 |
| REACTOME_MRNA_PROCESSING | 1.878 | 0.0099 | 0.0523 |
| PID_IGF1_PATHWAY | 1.877 | 0.0141 | 0.0521 |
| SIG_INSULIN_RECEPTOR_PATHWAY_IN_CARDIAC_MYOCYTES | 1.876 | 0.0134 | 0.0522 |
| KEGG_B_CELL_RECEPTOR_SIGNALING_PATHWAY | 1.870 | 0.0039 | 0.0535 |
| REACTOME_INNATE_IMMUNE_SYSTEM | 1.865 | 0.0098 | 0.0547 |
| KEGG_PROSTATE_CANCER | 1.863 | 0.0100 | 0.0551 |
| PID_FAK_PATHWAY | 1.862 | 0.0143 | 0.0548 |
| REACTOME_RESPONSE_TO_ELEVATED_PLATELET_CYTOSOLIC_CA2_ | 1.854 | 0.0121 | 0.0571 |
| REACTOME_ACTIVATED_TLR4_SIGNALLING | 1.848 | 0.0106 | 0.0588 |
| BIOCARTA_TH1TH2_PATHWAY | 1.848 | 0.0103 | 0.0584 |
| BIOCARTA_ASBCCELL_PATHWAY | 1.843 | 0.0039 | 0.0597 |
| REACTOME_PROCESSING_OF_CAPPED_INTRON_CONTAINING_PRE_MRNA | 1.843 | 0.0078 | 0.0594 |
| PID_IL4_2PATHWAY | 1.841 | 0.0099 | 0.0598 |
| REACTOME_TRAF6_MEDIATED_INDUCION_OF_NFKB_AND_MAP_KINASES_UPON_TLR7_8_OR_9_ACTIVATION | 1.839 | 0.0243 | 0.0599 |
| PID_TCPTP_PATHWAY | 1.833 | 0.0138 | 0.0613 |
| REACTOME_IL_RECEPTOR_SHC_SIGNALING | 1.831 | 0.0121 | 0.0618 |
| KEGG_VIRAL_MYOCARDITIS | 1.816 | 0.0158 | 0.0664 |
| REACTOME_CELL_SURFACE_INTERACTIONS_AT_THE_VASCULAR_WALL | 1.808 | 0.0183 | 0.0692 |
| ST_INTEGRIN_SIGNALING_PATHWAY | 1.808 | 0.0104 | 0.0688 |
| REACTOME_CYTOSOLIC_TRNA_AMINOACYLATION | 1.806 | 0.0178 | 0.0688 |
| BIOCARTA_GSK3_PATHWAY | 1.799 | 0.0247 | 0.0711 |
| PID_IL2_PI3KPATHWAY | 1.790 | 0.0117 | 0.0743 |
| REACTOME_GASTRIN_CREB_SIGNALLING_PATHWAY_VIA_PKC_AND_MAPK | 1.788 | 0.0144 | 0.0749 |
| REACTOME_NUCLEOTIDE_BINDING_DOMAIN_LEUCINE_RICH_REPEAT_CONTAINING_RECEPTOR_NLR_SIGNALING_PATHWAYS | 1.786 | 0.0177 | 0.0753 |
| REACTOME_CLEAVAGE_OF_GROWING_TRANSCRIPT_IN_THE_TERMINATION_REGION_ | 1.785 | 0.0253 | 0.0752 |
| REACTOME_G_ALPHA1213_SIGNALLING_EVENTS | 1.785 | 0.0139 | 0.0748 |
| MIPS_SPLICEOSOME | 1.785 | 0.0208 | 0.0744 |

| | | | |
|--|-------|--------|--------|
| KEGG_BLADDER_CANCER | 1.779 | 0.0118 | 0.0764 |
| PID_CDC42_PATHWAY | 1.778 | 0.0223 | 0.0762 |
| REACTOME_TRIF_MEDIATED_TLR3_SIGNALING | 1.777 | 0.0255 | 0.0760 |
| PID_TRKRPATHWAY | 1.759 | 0.0241 | 0.0835 |
| BIOCARTA_CTLA4_PATHWAY | 1.757 | 0.0137 | 0.0840 |
| BIOCARTA_HER2_PATHWAY | 1.751 | 0.0230 | 0.0862 |
| BIOCARTA_GATA3_PATHWAY | 1.746 | 0.0249 | 0.0880 |
| BIOCARTA_ATM_PATHWAY | 1.745 | 0.0224 | 0.0879 |
| REACTOME_BASIGIN_INTERACTIONS | 1.743 | 0.0158 | 0.0881 |
| KEGG_NEUROTROPHIN_SIGNALING_PATHWAY | 1.742 | 0.0230 | 0.0880 |
| KEGG_P53_SIGNALING_PATHWAY | 1.738 | 0.0173 | 0.0895 |
| KEGG_ARRHYTHMOGENIC_RIGHT_VENTRICULAR_CARDIOMYOPATHY_ARVC | 1.737 | 0.0182 | 0.0893 |
| BIOCARTA_CD40_PATHWAY | 1.737 | 0.0209 | 0.0892 |
| REACTOME_JNK_C_JUN_KINASES_PHOSPHORYLATION_AND_ACTIVATION_MEDIATED_BY_ACTIVATED_HUMAN_TAK1 | 1.734 | 0.0177 | 0.0897 |
| REACTOME_TOLL_RECEPTOR_CASCADES | 1.732 | 0.0207 | 0.0905 |
| KEGG_PATHOGENIC_ESCHERICHIA_COLI_INFECTION | 1.729 | 0.0195 | 0.0912 |
| BIOCARTA_P53HYPOXIA_PATHWAY | 1.724 | 0.0280 | 0.0927 |
| PID_CIRCADIANPATHWAY | 1.721 | 0.0181 | 0.0940 |
| BIOCARTA_PTDINS_PATHWAY | 1.719 | 0.0321 | 0.0941 |
| MIPS_TNF_ALPHA_NF_KAPPA_B_SIGNALING_COMPLEX_3 | 1.705 | 0.0327 | 0.1007 |
| PID_GMCSF_PATHWAY | 1.705 | 0.0290 | 0.1002 |
| ST_PHOSPHOINOSITIDE_3_KINASE_PATHWAY | 1.692 | 0.0195 | 0.1060 |
| REACTOME_FORMATION_OF_TUBULIN_FOLDING_INTERMEDIATES_BY_CCT_TRIC | 1.688 | 0.0298 | 0.1076 |
| PID_CXCR4_PATHWAY | 1.687 | 0.0261 | 0.1076 |
| BIOCARTA_RANKL_PATHWAY | 1.679 | 0.0342 | 0.1114 |
| PID_THROMBIN_PAR1_PATHWAY | 1.675 | 0.0408 | 0.1130 |
| BIOCARTA_IL6_PATHWAY | 1.673 | 0.0351 | 0.1133 |
| REACTOME_PLATELET_AGGREGATION_PLUG_FORMATION | 1.673 | 0.0192 | 0.1131 |
| REACTOME_MRNA_SPLICING | 1.671 | 0.0395 | 0.1133 |
| ST_T_CELL_SIGNAL_TRANSDUCTION | 1.671 | 0.0329 | 0.1130 |
| KEGG_PANCREATIC_CANCER | 1.671 | 0.0370 | 0.1125 |
| BIOCARTA_TALL1_PATHWAY | 1.667 | 0.0348 | 0.1136 |
| PID_RET_PATHWAY | 1.659 | 0.0235 | 0.1173 |
| PID_VEGFR1_2_PATHWAY | 1.652 | 0.0439 | 0.1209 |
| REACTOME_NCAM_SIGNALING_FOR_NEURITE_OUT_GROWTH | 1.652 | 0.0308 | 0.1206 |
| KEGG_HYPERTROPHIC_CARDIOMYOPATHY_HCM | 1.651 | 0.0381 | 0.1204 |
| REACTOME_IL_2_SIGNALING | 1.651 | 0.0416 | 0.1200 |
| PID_AR_NONGENOMIC_PATHWAY | 1.649 | 0.0375 | 0.1201 |
| ST_B_CELL_ANTIGEN_RECEPTOR | 1.647 | 0.0371 | 0.1210 |
| BIOCARTA_RACCYCD_PATHWAY | 1.642 | 0.0304 | 0.1237 |
| REACTOME_CLASS_B_2_SECRETIN_FAMILY_RECEPTORS | 1.633 | 0.0359 | 0.1285 |
| REACTOME_PERK_REGULATED_GENE_EXPRESSION | 1.624 | 0.0475 | 0.1336 |

| | | | |
|--|-------|--------|--------|
| PID_INSULIN_GLUKOSE_PATHWAY | 1.624 | 0.0372 | 0.1331 |
| PID_CERAMIDE_PATHWAY | 1.621 | 0.0498 | 0.1343 |
| PID_NCADHERINPATHWAY | 1.620 | 0.0428 | 0.1346 |
| SIG_REGULATION_OF_THE_ACTIN_CYTOSKELETON_BY_RHO_GTPASES | 1.617 | 0.0493 | 0.1358 |
| REACTOME_DEVELOPMENTAL_BIOLOGY | 1.615 | 0.0432 | 0.1361 |
| MIPS_DGCR8_MULTIPROTEIN_COMPLEX | 1.608 | 0.0505 | 0.1402 |
| REACTOME_ACTIVATED_TAK1_MEDIATES_P38_MAPK_ACTIVATION | 1.603 | 0.0589 | 0.1431 |
| BIOCARTA_IL3_PATHWAY | 1.599 | 0.0503 | 0.1447 |
| ST_ERK1_ERK2_MAPK_PATHWAY | 1.599 | 0.0397 | 0.1441 |
| PID_IL8CXCR1_PATHWAY | 1.599 | 0.0443 | 0.1437 |
| BIOCARTA_HSP27_PATHWAY | 1.598 | 0.0367 | 0.1436 |
| PID_ARF6DOWNSTREAMPATHWAY | 1.593 | 0.0521 | 0.1465 |
| BIOCARTA_TNFR2_PATHWAY | 1.588 | 0.0306 | 0.1493 |
| PID_THROMBIN_PAR4_PATHWAY | 1.587 | 0.0614 | 0.1488 |
| PID_LYMPHANGIOGENESIS_PATHWAY | 1.583 | 0.0581 | 0.1511 |
| KEGG_GAP_JUNCTION | 1.582 | 0.0619 | 0.1513 |
| REACTOME_ACTIVATION_OF_CHAPERONES_BY_ATF6_ALPHA | 1.581 | 0.0472 | 0.1515 |
| BIOCARTA_CDMAC_PATHWAY | 1.576 | 0.0535 | 0.1542 |
| BIOCARTA_GLEEVEC_PATHWAY | 1.576 | 0.0339 | 0.1539 |
| REACTOME_IMMUNE_SYSTEM | 1.564 | 0.0469 | 0.1621 |
| BIOCARTA_CREB_PATHWAY | 1.563 | 0.0477 | 0.1625 |
| ST_GA13_PATHWAY | 1.560 | 0.0581 | 0.1636 |
| REACTOME_NOD1_2_SIGNALING_PATHWAY | 1.558 | 0.0531 | 0.1649 |
| REACTOME_MRNA_3_END_PROCESSING | 1.557 | 0.0373 | 0.1643 |
| BIOCARTA_AGR_PATHWAY | 1.557 | 0.0639 | 0.1638 |
| BIOCARTA_MAPK_PATHWAY | 1.556 | 0.0593 | 0.1641 |
| REACTOME_TRANSPORT_TO_THE_GOLGI_AND_SUBSEQUENT_MODIFICATION | 1.550 | 0.0536 | 0.1679 |
| PID_EPHA2_FWDPATHWAY | 1.550 | 0.0435 | 0.1674 |
| REACTOME_G_ALPHA_S_SIGNALLING_EVENTS | 1.549 | 0.0509 | 0.1670 |
| PID_FGF_PATHWAY | 1.548 | 0.0663 | 0.1672 |
| BIOCARTA_ALK_PATHWAY | 1.543 | 0.0631 | 0.1704 |
| REACTOME_RIG_I_MDA5_MEDIATED_INDUCION_OF_IFN_ALPHA_BETA_PATHWAYS | 1.540 | 0.0635 | 0.1724 |
| MIPS_KINASE_MATURATION_COMPLEX_1 | 1.534 | 0.0781 | 0.1759 |
| PID_INTEGRIN_A4B1_PATHWAY | 1.533 | 0.0507 | 0.1766 |
| REACTOME_GLUKOSE_TRANSPORT | 1.529 | 0.0586 | 0.1788 |
| MIPS_CDC5L_COMPLEX | 1.524 | 0.0744 | 0.1819 |
| BIOCARTA_TPO_PATHWAY | 1.517 | 0.0774 | 0.1871 |
| KEGG_RENAL_CELL_CARCINOMA | 1.513 | 0.0830 | 0.1898 |
| BIOCARTA_ECM_PATHWAY | 1.509 | 0.0597 | 0.1923 |
| BIOCARTA_ARF_PATHWAY | 1.508 | 0.0758 | 0.1920 |
| PID_CD8TCRPATHWAY | 1.508 | 0.0669 | 0.1913 |
| PID_MAPKTRKPATHWAY | 1.507 | 0.0553 | 0.1912 |
| BIOCARTA_RNA_PATHWAY | 1.507 | 0.0646 | 0.1906 |

| | | | |
|--|-------|--------|--------|
| PID_LKB1_PATHWAY | 1.507 | 0.0593 | 0.1903 |
| PID_ECADHERIN_NASCENTAJ_PATHWAY | 1.505 | 0.0762 | 0.1910 |
| BIOCARTA_MPR_PATHWAY | 1.503 | 0.0752 | 0.1920 |
| REACTOME_INTEGRIN_ALPHAIIIB_BETA3_SIGNALING | 1.498 | 0.0679 | 0.1952 |
| PID_MET_PATHWAY | 1.494 | 0.0827 | 0.1985 |
| MIPS_HCF_1_COMPLEX | 1.493 | 0.0676 | 0.1984 |
| PID_A6B1_A6B4_INTEGRIN_PATHWAY | 1.492 | 0.0777 | 0.1989 |
| PID_NFAT_3PATHWAY | 1.488 | 0.0955 | 0.2018 |
| BIOCARTA_IGFIR_PATHWAY | 1.478 | 0.0738 | 0.2093 |
| BIOCARTA_ETS_PATHWAY | 1.475 | 0.0774 | 0.2116 |
| PID_NETRIN_PATHWAY | 1.472 | 0.0864 | 0.2138 |
| REACTOME_TRNA_AMINOACYLATION | 1.471 | 0.0823 | 0.2130 |
| BIOCARTA_ERK_PATHWAY | 1.469 | 0.0929 | 0.2144 |
| REACTOME_L1CAM_INTERACTIONS | 1.469 | 0.0720 | 0.2140 |
| REACTOME_PROLONGED_ERK_ACTIVATION_EVENTS | 1.466 | 0.1004 | 0.2154 |
| BIOCARTA_PDGF_PATHWAY | 1.465 | 0.0857 | 0.2152 |
| PID_PI3KPLCTRKPATWAY | 1.465 | 0.0630 | 0.2147 |
| REACTOME_AMYLOIDS | 1.464 | 0.0918 | 0.2144 |
| PID_P53DOWNSTREAMPATHWAY | 1.459 | 0.0829 | 0.2191 |
| KEGG_DILATED_CARDIOMYOPATHY | 1.455 | 0.0984 | 0.2218 |
| REACTOME_GLYCOLYSIS | 1.454 | 0.0761 | 0.2224 |
| REACTOME_RNA_POL_I_PROMOTER_OPENING | 1.454 | 0.0923 | 0.2217 |
| PID_IL1PATHWAY | 1.452 | 0.0812 | 0.2231 |
| PID_ECADHERIN_KERATINOCYTE_PATHWAY | 1.451 | 0.1143 | 0.2224 |
| REACTOME_MAPK_TARGETS_NUCLEAR_EVENTS_MEDIATED_BY_MAP_KINASES | 1.451 | 0.0822 | 0.2216 |
| REACTOME_ACTIVATION_OF_GENES_BY_ATF4 | 1.451 | 0.0873 | 0.2213 |
| PID_IL8CXCR2_PATHWAY | 1.450 | 0.1075 | 0.2216 |
| BIOCARTA_IL2_PATHWAY | 1.445 | 0.1091 | 0.2252 |
| REACTOME_NRAGE_SIGNALS_DEATH_THROUGH_JNK | 1.443 | 0.0870 | 0.2261 |
| REACTOME_THROMBIN_SIGNALLING_THROUGH_PROTEINASE_ACTIVATED_RECEPTORS_PARS | 1.442 | 0.0780 | 0.2268 |
| REACTOME_IL1_SIGNALING | 1.438 | 0.1025 | 0.2295 |
| REACTOME_TRANSPORT_OF_MATURE_MRNA_DERIVED_FROM_AN_INTRONLESS_TRANSCRIPT | 1.437 | 0.1020 | 0.2302 |
| BIOCARTA_INTEGRIN_PATHWAY | 1.431 | 0.0976 | 0.2350 |
| MIPS_TNF_ALPHA_NF_KAPPA_B_SIGNALING_COMPLEX_6 | 1.429 | 0.0958 | 0.2356 |
| REACTOME_DOWNSTREAM_TCR_SIGNALING | 1.427 | 0.1029 | 0.2369 |
| ST_P38_MAPK_PATHWAY | 1.426 | 0.1010 | 0.2364 |
| PID_IFNGPATHWAY | 1.426 | 0.0911 | 0.2362 |
| BIOCARTA_PARI_PATHWAY | 1.425 | 0.1036 | 0.2357 |
| KEGG_AMINOACYL_TRNA_BIOSYNTHESIS | 1.423 | 0.1018 | 0.2370 |
| KEGG_EPITHELIAL_CELL_SIGNALING_IN_HELICOBACTER_PYLORI_INFECTION | 1.420 | 0.0937 | 0.2395 |
| ST_DIFFERENTIATION_PATHWAY_IN_PC12_CELLS | 1.419 | 0.1086 | 0.2394 |
| PID_SMAD2_3NUCLEARPATHWAY | 1.417 | 0.1033 | 0.2400 |

| | | | |
|---|-------|--------|--------|
| BIOCARTA_TCR_PATHWAY | 1.414 | 0.0961 | 0.2424 |
| BIOCARTA_KERATINOCYTE_PATHWAY | 1.414 | 0.0984 | 0.2416 |
| BIOCARTA_NKCELLS_PATHWAY | 1.413 | 0.1130 | 0.2413 |
| REACTOME_ANTIGEN_PRESENTATION_FOLDING_ASSEMBLY_AND_PEPTIDE_LOADING_OF_CLASS_I_MHC | 1.412 | 0.1083 | 0.2419 |
| PID_S1P_S1P4_PATHWAY | 1.410 | 0.1022 | 0.2431 |
| REACTOME_INTERFERON_GAMMA_SIGNALING | 1.405 | 0.1040 | 0.2473 |
| MIPS_TNF_ALPHA_NF_KAPPA_B_SIGNALING_COMPLEX_5 | 1.405 | 0.0935 | 0.2466 |
| REACTOME_RNA_POL_II_TRANSCRIPTION | 1.404 | 0.1300 | 0.2469 |
| BIOCARTA_HCMV_PATHWAY | 1.404 | 0.0943 | 0.2462 |
| REACTOME_NUCLEAR_RECEPTOR_TRANSCRIPTION_PATHWAY | 1.402 | 0.1098 | 0.2469 |
| PID_PRLSIGNALINGEVENTSPATHWAY | 1.400 | 0.1138 | 0.2480 |
| BIOCARTA_BIOPEPTIDES_PATHWAY | 1.400 | 0.1133 | 0.2477 |
| KEGG_ADIPOCYTOKINE_SIGNALING_PATHWAY | 1.398 | 0.1063 | 0.2487 |

1150
1151
1152
1153
1154
1155
1156
1157
1158
1159
1160
1161
1162
1163
1164
1165
1166
1167
1168
1169
1170
1171
1172
1173
1174
1175
1176
1177
1178
1179
1180
1181
1182

1183 **Table S5. GSEA results (FDR < 0.25) for comparison of healthy control tetramer positive**
 1184 **to healthy control tetramer negative.**

| NAME | NES | NOM p-val | FDR q-val |
|--|--------|-----------|------------|
| REACTOME_SRP_DEPENDENT_COTRANSLATIONAL_PROTEIN_TARGETING_TO_MEMBRANE | 4.5784 | <0.001 | 1 <0.00 |
| REACTOME_PEPTIDE_CHAIN_ELONGATION | 4.4660 | <0.001 | 1 <0.00 |
| REACTOME_TRANSLATION | 4.4433 | <0.001 | 1 <0.00 |
| MIPS_RIBOSOME_CYTOPLASMIC | 4.4039 | <0.001 | 1 <0.00 |
| KEGG_RIBOSOME | 4.3425 | <0.001 | 1 <0.00 |
| REACTOME_METABOLISM_OF_PROTEINS | 4.3121 | <0.001 | 1 <0.00 |
| REACTOME_INFLUENZA_VIRAL_RNA_TRANSCRIPTION_AND_REPLICATION | 4.2863 | <0.001 | 1 <0.00 |
| REACTOME_3_UTR_MEDIATED_TRANSLATIONAL_REGULATION | 4.2010 | <0.001 | 1 <0.00 |
| REACTOME_INFLUENZA_LIFE_CYCLE | 3.9434 | <0.001 | 1 <0.00 |
| REACTOME_METABOLISM_OF_MRNA | 3.9010 | <0.001 | 1 <0.00 |
| REACTOME_METABOLISM_OF_RNA | 3.6973 | <0.001 | 1 <0.00 |
| REACTOME_NONSENSE_MEDIATED_DECAY_ENHANCED_BY_THE_EXON_JUNCTION_COMPLEX | 3.6825 | <0.001 | 1 <0.00 |
| MIPS_NOP56P_ASSOCIATED_PRE_RRNA_COMPLEX | 3.2647 | <0.001 | 1 <0.00 |
| MIPS_60S_RIBOSOMAL_SUBUNIT_CYTOPLASMIC | 3.1934 | <0.001 | 1 0.000 |
| REACTOME_ACTIVATION_OF_THE_MRNA_UPON_BINDING_OF_THE_CAP_BINDING_COMPLEX_AND_EIFS_AND_SUBSEQUENT_BINDING_TO_43S | 2.9852 | <0.001 | 2 0.000 |
| REACTOME_FORMATION_OF_THE_TERNARY_COMPLEX_AND_SUBSEQUENTLY_THE_43S_COMPLEX | 2.9110 | <0.001 | 2 0.000 |
| MIPS_40S_RIBOSOMAL_SUBUNIT_CYTOPLASMIC | 2.8496 | <0.001 | 5 0.001 |
| REACTOME_IMMUNE_SYSTEM | 2.6550 | <0.001 | 4 0.003 |
| REACTOME_ADAPTIVE_IMMUNE_SYSTEM | 2.5564 | <0.001 | 3 0.003 |
| MIPS_TRBP_CONTAINING_COMPLEX_1 | 2.5334 | <0.001 | 8 0.007 |
| REACTOME_ANTIGEN_PROCESSING_CROSS_PRESENTATION | 2.4612 | <0.001 | 2 0.007 |
| PID_CXCR4_PATHWAY | 2.4525 | <0.001 | 4 0.008 |
| KEGG_PARKINSONS_DISEASE | 2.4241 | <0.001 | 3 0.011 |
| REACTOME_SIGNALING_BY_WNT | 2.3765 | 0.0020 | 1 0.011 |
| REACTOME_CTLA4_INHIBITORY_SIGNALING | 2.3647 | <0.001 | 7 0.012 |
| REACTOME_MRNA_SPLICING | 2.3517 | 0.0019 | 6 0.014 |
| BIOCARTA_ERK_PATHWAY | 2.3293 | <0.001 | 0 0.013 |
| REACTOME_INTERFERON_SIGNALING | 2.3281 | <0.001 | 6 0.015 |
| REACTOME_AUTODEGRADATION_OF_CDH1_BY_CDH1_APC_C | 2.3079 | <0.001 | 2 0.015 |
| REACTOME_CLASS_I_MHC_MEDIATED_ANTIGEN_PROCESSING_PRESENTATION | 2.3024 | <0.001 | 3 0.015 |
| REACTOME_ER_PHAGOSOME_PATHWAY | 2.3011 | 0.0020 | 0 0.016 |
| REACTOME_APC_C_CDC20_MEDIATED_DEGRADATION_OF_MITOTIC_PROTEINS | 2.2783 | <0.001 | 6 |

| | | | |
|--|--------|--------|------------|
| REACTOME_PROCESSING_OF_CAPPED_INTRON_CONTAINING_PRE_MRNA | 2.2775 | <0.001 | 0.016 2 |
| REACTOME_MRNA_PROCESSING | 2.2308 | 0.0020 | 0.021 7 |
| MIPS_55S_RIBOSOME_MITOCHONDRIAL | 2.1984 | <0.001 | 0.027 0 |
| REACTOME_CELL_CYCLE_MITOTIC | 2.1896 | 0.0043 | 0.028 0 |
| KEGG_OXIDATIVE_PHOSPHORYLATION | 2.1375 | 0.0020 | 0.038 4 |
| PID_TELOMERASEPATHWAY | 2.1303 | 0.0021 | 0.039 4 |
| REACTOME_HOST_INTERACTIONS_OF_HIV_FACTORS | 2.1297 | 0.0040 | 0.038 5 |
| REACTOME_COSTIMULATION_BY_THE_CD28_FAMILY | 2.0994 | 0.0020 | 0.045 0 |
| REACTOME_MITOTIC_PROMETAPHASE | 2.0919 | <0.001 | 0.046 0 |
| KEGG_SPLICEOSOME | 2.0764 | 0.0020 | 0.049 6 |
| REACTOME_MEMBRANE_TRAFFICKING | 2.0732 | 0.0084 | 0.049 8 |
| MIPS_PA28_20S_PROTEASOME | 2.0694 | 0.0039 | 0.049 6 |
| REACTOME_P53_INDEPENDENT_G1_S_DNA_DAMAGE_CHECKPOINT | 2.0686 | 0.0041 | 0.048 6 |
| REACTOME_APOPTOSIS | 2.0643 | 0.0036 | 0.048 7 |
| REACTOME_DESTABILIZATION_OF_MRNA_BY_AUF1_HNRNP_D0 | 2.0556 | <0.001 | 0.050 8 |
| REACTOME_RESPIRATORY_ELECTRON_TRANSPORT_ATP_SYNTHESIS_BY_CHEMIOSMOTIC_C OUPLING_AND_HEAT_PRODUCTION_BY_UNCOUPLING_PROTEINS_ | 2.0501 | 0.0061 | 0.051 2 |
| KEGG_PRIMARY_IMMUNODEFICIENCY | 2.0356 | 0.0042 | 0.055 4 |
| REACTOME_HIV_INFECTION | 2.0339 | 0.0021 | 0.055 0 |
| REACTOME_REGULATION_OF_MITOTIC_CELL_CYCLE | 2.0319 | 0.0041 | 0.054 6 |
| REACTOME_REGULATION_OF_MRNA_STABILITY_BY_PROTEINS_THAT_BIND_AU_RICH_ELEM ENTS | 2.0100 | 0.0039 | 0.061 2 |
| MIPS_F1F0_ATP_SYNTHASE_MITOCHONDRIAL | 1.9992 | 0.0019 | 0.063 8 |
| MIPS_C_COMPLEX_SPLICEOSOME | 1.9984 | <0.001 | 0.062 8 |
| REACTOME_SCF_BETA_TRCP_MEDIATED_DEGRADATION_OF_EMII | 1.9931 | 0.0021 | 0.064 0 |
| REACTOME_MRNA_SPLICING_MINOR_PATHWAY | 1.9904 | 0.0040 | 0.063 7 |
| REACTOME_SYNTHESIS_OF_SUBSTRATES_IN_N_GLYCAN_BIOSYTHESIS | 1.9857 | 0.0058 | 0.064 4 |
| MIPS_26S_PROTEASOME | 1.9680 | 0.0057 | 0.070 1 |
| REACTOME_REGULATION_OF_APOPTOSIS | 1.9583 | 0.0083 | 0.073 3 |
| REACTOME_CROSS_PRESENTATION_OF_SOLUBLE_EXOGENOUS_ANTIGENS_ENDOSOMES | 1.9569 | 0.0041 | 0.072 7 |
| REACTOME_CLEAVAGE_OF_GROWING_TRANSCRIPT_IN_THE_TERMINATION_REGION_ | 1.9561 | 0.0097 | 0.071 9 |
| REACTOME_VIF_MEDIATED_DEGRADATION_OF_APOBEC3G | 1.9543 | 0.0059 | 0.071 6 |
| REACTOME_INTERFERON_GAMMA_SIGNALING | 1.9356 | 0.0083 | 0.078 6 |
| REACTOME_CELL_CYCLE_CHECKPOINTS | 1.9337 | 0.0122 | 0.078 2 |
| REACTOME_APC_C_CDH1_MEDIATED_DEGRADATION_OF_CDC20_AND_OTHER_APC_C_CDH1_ TARGETED_PROTEINS_IN_LATE_MITOSIS_EARLY_G1 | 1.9316 | 0.0061 | 0.077 8 |
| MIPS_20S_PROTEASOME | 1.9260 | 0.0080 | 0.079 1 |
| REACTOME_DEADENYLATION_OF_MRNA | 1.9129 | 0.0061 | 0.084 4 |

| | | | |
|---|--------|--------|-------|
| REACTOME_AUTODEGRADATION_OF_THE_E3_UBIQUITIN_LIGASE_COPI | 1.9110 | 0.0122 | 0.084 |
| | | | 2 |
| REACTOME_FORMATION_OF_ATP_BY_CHEMIOSMOTIC_COUPLING | 1.9053 | 0.0038 | 0.085 |
| | | | 7 |
| REACTOME_ASSEMBLY_OF_THE_PRE_REPLICATIVE_COMPLEX | 1.8950 | 0.0140 | 0.089 |
| | | | 6 |
| REACTOME_PREFOLDIN_MEDIATED_TRANSFER_OF_SUBSTRATE_TO_CCT_TRIC | 1.8841 | 0.0109 | 0.094 |
| | | | 4 |
| REACTOME_REGULATION_OF_ORNITHINE_DECARBOXYLASE_ODC | 1.8813 | 0.0196 | 0.094 |
| | | | 5 |
| REACTOME_ANTIGEN_PRESENTATION_FOLDING_ASSEMBLY_AND_PEPTIDE_LOADING_OF_CLASS_I_MHC | 1.8812 | 0.0101 | 0.093 |
| | | | 3 |
| REACTOME_PROTEIN_FOLDING | 1.8799 | 0.0118 | 0.092 |
| | | | 7 |
| MIPS_SPLICEOSOME | 1.8724 | 0.0096 | 0.095 |
| | | | 5 |
| KEGG_PATHOGENIC_ESCHERICHIA_COLI_INFECTION | 1.8644 | 0.0102 | 0.098 |
| | | | 0 |
| REACTOME_FORMATION_OF_TUBULIN_FOLDING_INTERMEDIATES_BY_CCT_TRIC | 1.8609 | 0.0061 | 0.098 |
| | | | 4 |
| REACTOME_CELL_CYCLE | 1.8472 | 0.0180 | 0.104 |
| | | | 2 |
| REACTOME_APC_CDC20_MEDIATED_DEGRADATION_OF_NEK2A | 1.8331 | 0.0220 | 0.111 |
| | | | 3 |
| REACTOME_CDK_MEDIATED_PHOSPHORYLATION_AND_REMOVAL_OF_CDC6 | 1.8210 | 0.0104 | 0.117 |
| | | | 7 |
| REACTOME_ANTIGEN_PROCESSING_UBIQUITINATION_PROTEASOME_DEGRADATION | 1.8157 | 0.0142 | 0.119 |
| | | | 9 |
| KEGG_PROTEASOME | 1.8124 | 0.0101 | 0.120 |
| | | | 7 |
| REACTOME_P53_DEPENDENT_G1_DNA_DAMAGE_RESPONSE | 1.8077 | 0.0161 | 0.121 |
| | | | 9 |
| REACTOME_LOSS_OF_NLP_FROM_MITOTIC_CENTROSOMES | 1.7845 | 0.0136 | 0.136 |
| | | | 8 |
| REACTOME_MRNA_3_END_PROCESSING | 1.7772 | 0.0044 | 0.140 |
| | | | 4 |
| MIPS_PA700_20S_PA28_COMPLEX | 1.7735 | 0.0123 | 0.141 |
| | | | 2 |
| REACTOME_CYCLIN_E_ASSOCIATED_EVENTS_DURING_G1_S_TRANSITION | 1.7688 | 0.0288 | 0.143 |
| | | | 2 |
| REACTOME_TCA_CYCLE_AND_RESPIRATORY_ELECTRON_TRANSPORT | 1.7638 | 0.0200 | 0.145 |
| | | | 5 |
| KEGG_NITROGEN_METABOLISM | 1.7591 | 0.0133 | 0.147 |
| | | | 1 |
| KEGG_BLADDER_CANCER | 1.7570 | 0.0232 | 0.147 |
| | | | 2 |
| BIOCARTA_CTLA4_PATHWAY | 1.7537 | 0.0100 | 0.148 |
| | | | 2 |
| REACTOME_RESPIRATORY_ELECTRON_TRANSPORT | 1.7530 | 0.0292 | 0.147 |
| | | | 0 |
| REACTOME_METABOLISM_OF_AMINO_ACIDS_AND_DERIVATIVES | 1.7374 | 0.0218 | 0.157 |
| | | | 8 |
| REACTOME_TRANSPORT_TO_THE_GOLGI_AND_SUBSEQUENT_MODIFICATION | 1.7357 | 0.0343 | 0.157 |
| | | | 3 |
| REACTOME_CYTOKINE_SIGNALING_IN_IMMUNE_SYSTEM | 1.7297 | 0.0196 | 0.160 |
| | | | 1 |
| MIPS_CDC5L_COMPLEX | 1.7279 | 0.0242 | 0.159 |
| | | | 9 |
| KEGG_PROTEIN_EXPORT | 1.7275 | 0.0211 | 0.158 |
| | | | 6 |
| REACTOME_POST_TRANSLATIONAL_PROTEIN_MODIFICATION | 1.7270 | 0.0240 | 0.157 |
| | | | 5 |
| REACTOME ASPARAGINE_N_LINKED_GLYCOSYLATION | 1.7135 | 0.0252 | 0.167 |
| | | | 4 |
| REACTOME_CHOLESTEROL_BIOSYNTHESIS | 1.6956 | 0.0222 | 0.181 |
| | | | 3 |
| PID_IL3_PATHWAY | 1.6934 | 0.0287 | 0.181 |
| | | | 6 |
| REACTOME_CDT1_ASSOCIATION_WITH_THE_CDC6_ORC_ORIGIN_COMPLEX | 1.6927 | 0.0462 | 0.180 |
| | | | 4 |

| | | | |
|--|--------|--------|-------|
| REACTOME_GOLGI_ASSOCIATED_VESICLE_BIOGENESIS | 1.6876 | 0.0205 | 0.183 |
| | | | 8 |
| REACTOME_PHOSPHORYLATION_OF_CD3_AND_TCR_ZETA_CHAINS | 1.6875 | 0.0342 | 0.182 |
| | | | 1 |
| REACTOME_GENERATION_OF_SECOND_MESSENGER_MOLECULES | 1.6854 | 0.0205 | 0.182 |
| | | | 4 |
| REACTOME_ANTIVIRAL_MECHANISM_BY_IFN_STIMULATED_GENES | 1.6847 | 0.0297 | 0.181 |
| | | | 3 |
| MIPS_39S_RIBOSOMAL_SUBUNIT_MITOCHONDRIAL | 1.6812 | 0.0324 | 0.183 |
| | | | 0 |
| KEGG_CHEMOKINE_SIGNALING_PATHWAY | 1.6772 | 0.0367 | 0.185 |
| | | | 2 |
| REACTOME_IMMUNOREGULATORY_INTERACTIONS_BETWEEN_A_LYMPHOID_AND_A_NON_LYMPHOID_CELL | 1.6688 | 0.0400 | 0.191 |
| | | | 3 |
| BIOCARTA_IL2RB_PATHWAY | 1.6623 | 0.0347 | 0.195 |
| | | | 5 |
| REACTOME_MITOTIC_G1_G1_S_PHASES | 1.6586 | 0.0348 | 0.197 |
| | | | 4 |
| MIPS_TNF_ALPHA_NF_KAPPA_B_SIGNALING_COMPLEX_6 | 1.6576 | 0.0218 | 0.196 |
| | | | 8 |
| MIPS_28S_RIBOSOMAL_SUBUNIT_MITOCHONDRIAL | 1.6572 | 0.0315 | 0.195 |
| | | | 6 |
| REACTOME_APC_C_CDC20_MEDIATED_DEGRADATION_OF_CYCLIN_B | 1.6556 | 0.0345 | 0.195 |
| | | | 5 |
| REACTOME_ORC1_REMOVAL_FROM_CHROMATIN | 1.6472 | 0.0386 | 0.201 |
| | | | 8 |
| REACTOME_INHIBITION_OF_THE_PROTEOLYTIC_ACTIVITY_OF_APC_C_REQUIRED_FOR_THE_ONSET_OF_ANAPHASE_BY_MITOTIC_SPINDLE_CHECKPOINT_COMPONENTS | 1.6381 | 0.0270 | 0.209 |
| | | | 5 |
| BIOCARTA_BCELLSURVIVAL_PATHWAY | 1.6252 | 0.0414 | 0.221 |
| | | | 2 |
| BIOCARTA_PROTEASOME_PATHWAY | 1.6242 | 0.0227 | 0.220 |
| | | | 5 |
| KEGG_REGULATION_OF_ACTIN_CYTOSKELETON | 1.6228 | 0.0425 | 0.220 |
| | | | 0 |
| PID_IL8CXCR2_PATHWAY | 1.6211 | 0.0454 | 0.219 |
| | | | 9 |
| REACTOME_CTNNB1_PHOSPHORYLATION_CASCADE | 1.6209 | 0.0387 | 0.218 |
| | | | 2 |
| REACTOME_RNA_POL_II_TRANSCRIPTION | 1.6194 | 0.0417 | 0.218 |
| | | | 1 |
| BIOCARTA_EIF_PATHWAY | 1.6178 | 0.0476 | 0.218 |
| | | | 1 |
| REACTOME_POST_CHAPERONIN_TUBULIN_FOLDING_PATHWAY | 1.6122 | 0.0528 | 0.222 |
| | | | 0 |
| REACTOME_SCFSKP2_MEDIATED_DEGRADATION_OF_P27_P21 | 1.6112 | 0.0454 | 0.221 |
| | | | 5 |
| PID_TCR_PATHWAY | 1.6094 | 0.0431 | 0.221 |
| | | | 6 |
| REACTOME_MITOTIC_G2_G2_M_PHASES | 1.6030 | 0.0413 | 0.226 |
| | | | 6 |
| KEGG_ANTIGEN_PROCESSING_AND_PRESENTATION | 1.5905 | 0.0626 | 0.238 |
| | | | 9 |
| PID_IL6_7PATHWAY | 1.5888 | 0.0422 | 0.239 |
| | | | 0 |
| REACTOME_CONVERSION_FROM_APC_C_CDC20_TO_APC_C_CDH1_IN_LATE_ANAPHASE | 1.5860 | 0.0398 | 0.240 |
| | | | 5 |
| BIOCARTA_MTOR_PATHWAY | 1.5772 | 0.0530 | 0.248 |
| | | | 4 |
| REACTOME_PHOSPHORYLATION_OF_THE_APC_C | 1.5754 | 0.0494 | 0.248 |
| | | | 5 |
| PID_GMCSF_PATHWAY | 1.5735 | 0.0575 | 0.248 |
| | | | 7 |
| KEGG_PROGESTERONE_MEDIATED_OOCYTE_MATURATION | 1.5725 | 0.0447 | 0.247 |
| | | | 8 |

1185
1186
1187
1188
1189

Table S6: Curated gene signatures corresponding to Figure 4C.

| Gene Set | Description | Reference | Gene Symbols |
|---|--|-------------------|--|
| MOG induced EAE ⁺ | Gene signature comprised of differentially expressed genes in MOG induced EAE in rats. | (37) | See Supplementary Table 4. |
| Th1 signature ⁺ | Th1-specific gene signature derived from C57BL/6 mice. | (38) | See Supplementary Table 4. |
| Th2 signature ⁺ | Th2-specific gene signature derived from C57BL/6 mice. | (38) | See Supplementary Table 4. |
| Th17 signature ⁺ | Th17-specific gene signature derived from C57BL/6 mice. | (38) | See Supplementary Table 4. |
| Pathogenic Th17 ⁺ | Pathogenic signature of Th17 cells derived by Lee et. al. | (16) | See Figure 4D for 23-list gene set. |
| Th17 differential expression ⁺ | Differentially expressed Th17 genes derived from comparison of Th17 cells induced with TGFb1 and IL-6 versus TGFb3 and IL-6. | (16) | See Supplementary Table 1. |
| Th17 cytokines | Cytokines up-regulated in mouse Th17 cells relative to Th0 cells. | (39) Figure 3B | IL23R, IL9, IL17R, IL17A, IL24, IL12RB1, IL17F, LIF, IL10, TNFRSF8, IL21, IL1R1 |
| Th17 combinatorial core | Combinatorial core of transcription factor targets involved in Th17 cell specification. | (39) Figure 6D | STAT3, IRF4, RORC, MAF, BATF, FOSL2, CYSLTR2, CCL5, HIF1A, IL18RAP, IL17A, IL17F, CCL20, CCR8, IL2, CXCR3, TBX21, CCL4, CCL3, CCR6, IL1R1, GPR15, IL18R1, IL21RB1, IL7R, IL2RA, LTB4R1, IL12RB2, LTB, IL10RA, SMAD3, IL23A, CCR7, IL24, IL4RA, IL21, CXCL10, IL6RA, IL16 |
| PLP induced EAE ⁺ | Gene signature comprised of differentially expressed genes in PLP induced EAE (SJL/J mice). | (35) | See Supplementary Table 5. |
| Th17.1 EM selective | Th17.1 effector memory selective genes identified using FACs-sorted and <i>ex-vivo</i> stimulated human CD4 ⁺ CD25 ⁻ CRTH2 ⁻ CCR7 ^{lo} CCR6 ⁺ CCR4 ^{lo} CXCR3 ^{hi} cells. | (40) Table S1 | ME1, ENPP1, ADAM23, COLQ, SLC4A10, CA2, SCRNI, ABCB1, CLEC2B, CCR2, DPP4, KLRB1 |
| Th17 EM core | Th17 effector memory core genes identified using FACs-sorted and <i>ex-vivo</i> stimulated human CD4 ⁺ CD25 ⁻ CRTH2 ⁻ CCR7 ^{lo} CCR6 ⁺ CCR4 ^{lo} CXCR3 ^{hi} cells. | (40) Table S1 | IL17RE, PIK3R6, HLF, CCR6, RORC, CTSH, LRP12, CHN1, HPGD, ADAM12, PTPN13 |
| MDR1 Th17.1 EM in Crohn's patients | <i>Ex vivo</i> transcriptional signature of MDR1 ⁺ Th17.1 effector memory cells isolated from Crohn's disease patient lesions. | (40) Table S2 | ABCB1, ND6, GNLY, CDR1, CCL5, IL2, ADAM23, MALAT1, CA2, LRRN3, IL22, GPR15, DSE, IL18RAP, CCL20, GAB3, PELO, ARHGEF4, CSF2, PDE4DIP, SLC4A10, TUBB2A, MIR221, CDC42EP5, MYBL1, SYTL2, FERMT2, B3GALT2, RPL41, PRF1, PLCB1, TLE1, AUTS2, ERN1, CXCR6, IL23R, LGALS3 |
| Th17 EM selective | Th17.1 EM specific genes of FACs-sorted and <i>ex-vivo</i> stimulated human CD4 ⁺ CD25 ⁻ CRTH2 ⁻ CCR7 ^{lo} CCR6 ⁺ CCR4 ^{lo} CXCR3 ^{hi} cells. | (40) Table S1 | SHF, IL17A, IL17F, ATP1B1, S100A4, NTRK2, PLD1, PPARG, ITGAE, PAK3, TMOD1, IL26, TIMP4, HRH4, TIMP1 |

⁺For gene sets derived from rat or mice, gene symbols were mapped using HGNC gene checker.

1193
1194

Table S7. Gene sets used for leading edge analysis to define pathogenic gene signature.

| NAME | SIZE | NES | FDR q-val |
|--|------|--------|-----------|
| KEGG_CYTOKINE_CYTOKINE_RECEPTOR_INTERACTION | 87 | 5.2552 | <0.001 |
| PID_NFAT_TFPATHWAY | 39 | 3.7971 | <0.001 |
| BIOCARTA_CYTOKINE_PATHWAY | 12 | 3.5986 | <0.001 |
| REACTOME_GPCR_LIGAND_BINDING | 53 | 3.5342 | <0.001 |
| REACTOME_CLASS_A1_RHODOPSIN_LIKE_RECEPTORS | 43 | 3.4971 | <0.001 |
| PID_API1_PATHWAY | 44 | 3.3188 | <0.001 |
| PID_ATF2_PATHWAY | 32 | 3.2134 | <0.001 |
| REACTOME_GPCR_DOWNSTREAM_SIGNALING | 106 | 3.1118 | 0.0001 |
| REACTOME_SIGNALING_BY_GPCR | 139 | 3.0468 | 0.0001 |
| REACTOME_CHEMOKINE_RECEPTORS_BIND_CHEMOKINES | 21 | 3.0431 | 0.0001 |
| PID_TCRCALCIUMPATHWAY | 20 | 2.9931 | 0.0001 |
| REACTOME_PEPTIDE_LIGAND_BINDING_RECEPTORS | 27 | 2.8743 | 0.0001 |
| PID_IL23PATHWAY | 24 | 2.7896 | 0.0002 |
| PID_REG_GR_PATHWAY | 53 | 2.7694 | 0.0002 |
| KEGG_TYPE_I_DIABETES_MELLITUS | 22 | 2.6357 | 0.0008 |
| PID_SYNDECAN_2_PATHWAY | 22 | 2.0995 | 0.0215 |
| BIOCARTA_TOB1_PATHWAY | 16 | 2.0789 | 0.0234 |

1195
1196
1197
1198
1199
1200
1201
1202
1203
1204
1205
1206
1207
1208
1209
1210
1211
1212
1213
1214
1215
1216
1217
1218
1219
1220

1221 **Table S8. Summary of networks constructed by IPA from pathogenic signature.** Networks
 1222 1,2 and 8 were merged for subsequent analysis in figure 4D and networks 3-7 were merged for
 1223 presentation in figure S15.
 1224

| Network ID | Score | Number Focus Molecules | Top Diseases and Functions |
|------------|-------|------------------------|--|
| 1 | 56 | 29 | Cell Signaling, Molecular Transport, Vitamin and Mineral Metabolism |
| 2 | 41 | 23 | Cellular Development, Hematological System Development and Function, Hematopoiesis |
| 3 | 38 | 22 | Cellular Development, Cellular Growth and Proliferation, Hematological System Development and Function |
| 4 | 31 | 19 | Cell Signaling, Molecular Transport, Vitamin and Mineral Metabolism |
| 5 | 31 | 19 | Endocrine System Disorders, Gastrointestinal Disease, Metabolic Disease |
| 6 | 31 | 19 | Cell Cycle, Amino Acid Metabolism, Post-Translational Modification |
| 7 | 31 | 21 | Cell Death and Survival, Cellular Development, Hematopoiesis |
| 8 | 26 | 17 | Immunological Disease, Inflammatory Disease, Inflammatory Response |
| 9 | 20 | 15 | Cellular Movement, Hematological System Development and Function, Immune Cell Trafficking |
| 10 | 17 | 12 | Cell Death and Survival, Hematological System Development and Function, Immune Cell Trafficking |
| 11 | 16 | 12 | Cell Death and Survival, Cellular Compromise, Cellular Assembly and Organization |
| 12 | 15 | 11 | Cell Cycle, Gastrointestinal Disease, Organismal Injury and Abnormalities |
| 13 | 2 | 1 | Cell Death and Survival, Connective Tissue Development and Function, Gene Expression |
| 14 | 1 | 1 | Cancer, Reproductive System Disease, Lymphoid Tissue Structure and Development |

1225
 1226